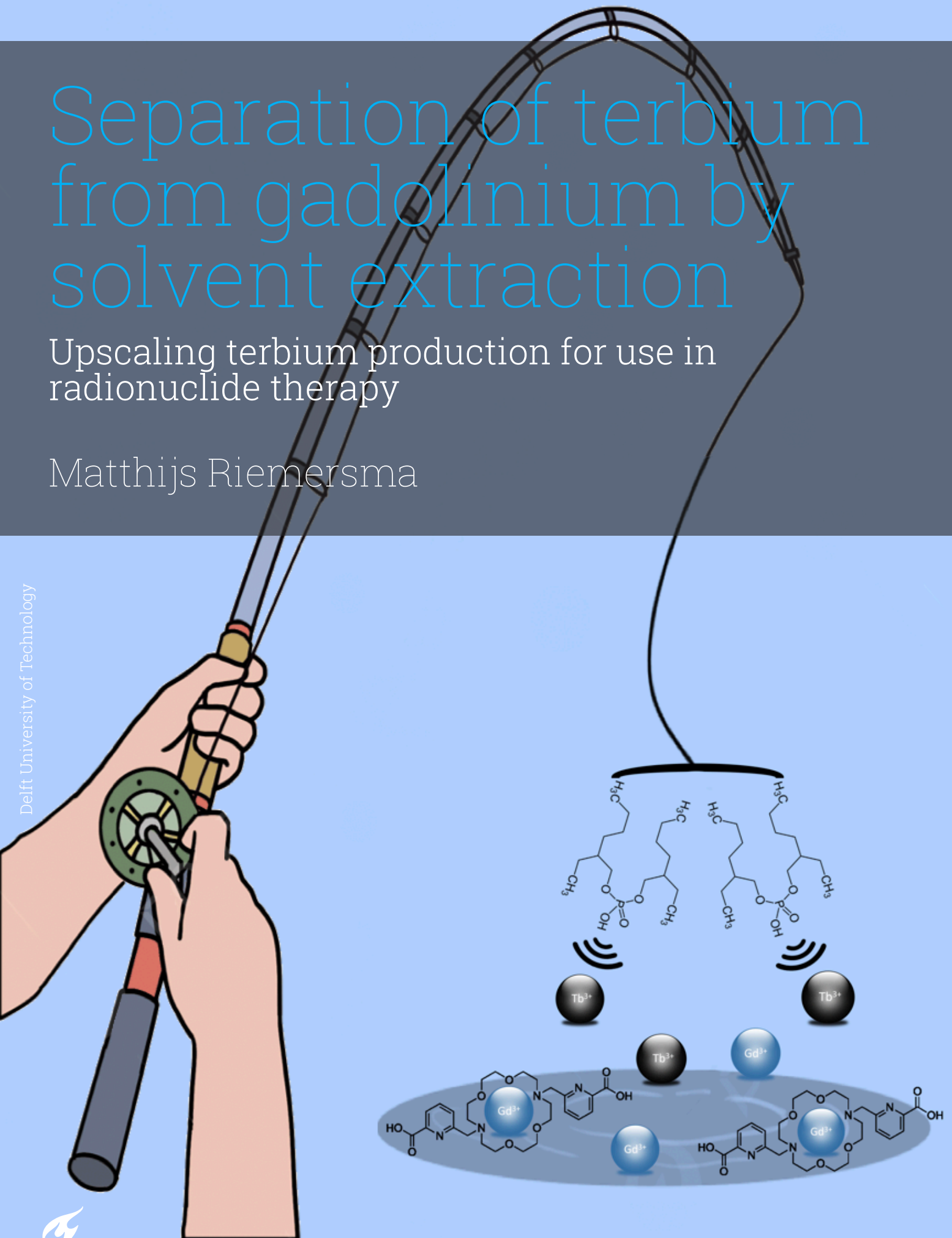


Separation of terbium from gadolinium by solvent extraction

Upscaling terbium production for use in radionuclide therapy

Matthijs Riemersma

Delft University of Technology



Separation of terbium from gadolinium by solvent extraction

Upscaling terbium production for use in
radionuclide therapy

by

Matthijs Riemersma

to obtain the degree of Master of Science
at the Delft University of Technology,
to be defended publicly on Friday June 7, 2024 at 14:00 PM.

Student number: 4689615
Project duration: October 23, 2023 – June 7, 2024
Thesis committee: Dr. ir. R. de Kruijff, TU Delft, supervisor
Dr. ir. A. G. Denkova, TU Delft
Dr. ir. M. Rohde, TU Delft

This thesis is confidential and cannot be made public until June 7, 2029.

An electronic version of this thesis is available at <http://repository.tudelft.nl/>.

Abstract

^{161}Tb is considered a promising alternative to ^{177}Lu in the treatment of neuroendocrine tumors and prostate cancer.¹⁻⁶ It is produced via neutron irradiation of ^{160}Gd targets and its subsequent separation from said targets. Current separation methods have limitations so a fast removal method of the Gd bulk is desired. Such a method is developed in this research using solvent extraction techniques. Three extractants were investigated, the one with the highest potential, DEHPA, was used to optimize the extraction. This yielded a Tb extraction efficiency of $98.6 \pm 0.2 \%$ and a Gd extraction efficiency of $85.7 \pm 5.5 \%$ followed by a Tb back-extraction efficiency of $98.2 \pm 0.1 \%$ and a Gd back-extraction efficiency of more than $98.2 \pm 0.1 \%$. The Tb/Gd separation was increased by adding the reverse size selective chelator MACROPA to the aqueous phase to preferentially complex Gd in the aqueous phase. This yielded a Tb and Gd extraction efficiency of $95.0 \pm 0.2 \%$ and $53.1 \pm 3.0 \%$ respectively. The ratio between total EEs of Tb and Gd after three subsequent extractions was approximately 10 demonstrating the potential of using sequential extractions to remove a bulk of Gd from Tb. The procedure of doing consecutive extractions must however be further optimized as nearly 80% of Tb was not extracted. Finally, it was shown that the resulting solution after bulk Gd removal can still be further purified using an ion exchange column. In future research, it is highly advised to investigate the recycling of Gd and MACROPA from the aqueous phase after extraction to allow for further irradiation of the Gd and re-usability of the MACROPA.

List of Abbreviations

Positron emission tomography	PET
Single-photon emission computed tomography	SPECT
Inductively coupled plasma mass spectrometry	ICP-MS
Ultraviolet–visible	UV-Vis
Single-strand break	SSB
Double-strand break	DSB
Linear energy transfer	LET
Electron capture	EC
Internal conversion	IC
Extraction efficiency	EE
Separation factor	SF
Back-extraction efficiency	BEE
Rare-earth metal	REE
Di-(2-ethylhexyl)-phosphoric acid	DEHPA/HDEHP
2-ethylhexylphosphonic acid	HEHPA/HEHEHP/PC-88A
Tributyl-phosphate	TBP
Dodecyl-phosphonic acid	DDPA
Thallium-activated sodium iodine detector	Nal(Tl) detector
Instant thin layer chromatography	iTLC
High-pressure liquid chromatography	HPLC

List of Figures

2.2	A: A visualization of single-photon emission computed tomography (SPECT). A radionuclide emits photons from the site of a tumor that are absorbed by a scintillation crystal and then detected by a gamma camera behind a collimator that only allows the transfer of photons to the camera at right-angles. These rotate so that a 3D image can be made by a computer. B: A visualization of positron emission tomography (PET). The 511 keV photons resulting from annihilation of an emitted positron with an electron in the body are measured by a ring of detectors and an image is made by a computer. ²⁴	4
2.1	A visualization of the types of radiation (α , β and Auger electrons) in radionuclide therapy. The number of ionizations (*) is shown along the path (-) of the decay particles. γ -radiation is not shown. ²¹	4
2.3	A schematic overview of the chelation process. The metal M^{n+} forms a complex ML_n with ligand L which is highly hydrophobic and is therefore extracted to the organic phase.	5
2.4	A visualization of liquid-liquid extraction and subsequent back-extraction. The vial containing the organic phase with extractant and the aqueous phase with metal is vortexed to allow for faster complex formation. The phases are then separated after which a back-extracting agent is added to the vial with the organic phase to break the complex. Finally, the phases are separated again.	6
2.5	The DEHPA-lanthanide complex, DEHPA forms the complex as a dimer according to Equation 2.2. ⁶¹	8
2.6	The amount of complexed Tb and Gd ($[Gd] = 15$ mM and $[Tb] = 0.15$ mM) with 0.5 M MACROPA versus pH, as calculated by HYSS using the stability constants of MACROPA-lanthanide complexes as reported by Roca-Sabio et al. ⁶²	8
2.7	The ion exchange column chromatography process, first the sample mixture is loaded onto the column replacing the ions initially bounded. The column is then sequentially eluted with an increasingly higher salt elution buffer and the fractions are collected. The ions will come out of the columns in order of the strength with which they are bounded, from low to high resulting in their separation. ⁶⁸	9
2.8	An overview of the ICP-MS system. ⁷⁰	10
3.1	The DDPA/TBP solution. Not all DDPA has dissolved resulting in a cloudy solution with the undissolved DDPA powder at the bottom of the vial.	13
3.2	1: Loading/elution solution, 2: Tubing, 3: Pump, 4: Purge tube for removing air, 5: Column inlet, 6: Column, 7: Column outlet, 8a: Tubing to waste container, 8b: Tubing to vials, 9: Fraction collector, 10: Collection vials.	16
4.1	Extraction efficiencies [%] of Tb and Gd for various extractants at pH = 1.3. The extractions were carried out with 15 mM Gd and 0.15 mM Tb in HNO_3 as the aqueous phase, PE 100-140 as the organic phase and 10 min vortexing time. The concentrations of the extractants are 0.1 M DEHPA, 0.5 M PC-88A and 0.1 M DDPA with 2 % v/v TBP. The error bars represent one standard deviation of the mean.	18
4.2	A: Extraction efficiency [%] of Tb for DEHPA and PC-88A at pH = 1.3 versus extractant concentration. Bottom: Extraction efficiencies [%] of Tb and Gd for 0.1 M DEHPA and 0.5 M PC-88A versus pH. All extractions were carried out with 15 mM Gd and 0.15 mM Tb in HNO_3 as the aqueous phase, PE 100-140 as the organic phase and 10 min vortexing time. The error bars represent one standard deviation of the mean.	19

4.3	Extraction efficiencies [%] of Tb and Gd using 0.1 M DEHPA at various pH values. The extractions were carried out with 15 mM Gd and 0.15 mM Tb in HNO ₃ as the aqueous phase, PE 100-140 as the organic phase and 10 min vortexing time. The error bars represent one standard deviation of the mean. The lines serve to guide the eyes but have no scientific meaning.	20
4.4	Extraction efficiencies [%] of Tb and Gd using 0.1 M DEHPA and aqueous phase at pH = 1.3. The extractions were carried out with 15 mM Gd and 0.15 mM Tb in HNO ₃ , PE 100-140 as the organic phase and various vortexing times. The error bars represent one standard deviation of the mean. The lines serve to guide the eyes but have no scientific meaning.	21
4.5	Extraction efficiency [%] of Tb and Gd using 0.1 M DEHPA in PE 100-140 with aqueous phase HNO ₃ or HCl at pH = 1.3. The extractions were carried out with 15 mM Gd and 0.15 mM Tb and 10 minutes vortexing time. The error bars represent one standard deviation of the mean.	22
4.6	Extraction efficiencies [%] of Tb and Gd. The extractions were carried out with 150 mM Gd and 0.15 mM Tb in HNO ₃ as the aqueous phase at pH = 1.3. Various concentrations of DEHPA in PE 100-140 were used as the organic phase and the vials were vortexed for 10 minutes. The error bars represent one standard deviation of the mean.	23
4.7	BEE % of Tb with various concentrations HNO ₃ as the back-extracting agent. The vortexing time was 10 minutes and the error bars represent one standard deviation of the mean. The lines serve to guide the eyes but have no scientific meaning.	24
4.8	BEE [%] of Tb with various concentrations HNO ₃ and HCl as the back-extracting agent. The vortexing time was 10 minutes and the error bars represent one standard deviation of the mean.	24
4.10	The simulated speciation results from Section 2.3.4 (right figure) next to the DEHPA extraction versus pH. The concentrations Tb and Gd are the same as in Figure 4.3, using 0.1 M DEHPA to extract and a simulated 0.5 M MACROPA to preferentially complex Gd in the aqueous phase. The lines in the left figure serve to guide the eyes but have no scientific meaning.	25
4.9	EEs of Tb and Gd using 0.005 M MACROPA and 0.001 M DEHPA and back-extraction with 2 M HNO ₃ for 100x diluted Tb/Gd aqueous solution at pH 2 and pH 3.5, a vortexing time of 10 min and PE 100-140 as the organic phase. The error bars represent one standard deviation of the mean.	25
4.12	EEs of Tb and Gd using MACROPA and 0.001 M DEHPA and back-extraction with 2 M HNO ₃ for 100x diluted Tb/Gd aqueous solution at pH 3.5, a vortexing time of 10 min and PE 100-140 as the organic phase versus various concentrations of MACROPA. The error bars represent one standard deviation of the mean.	26
4.11	The formation of a third phase after vortexing in experiments with higher concentrations MACROPA.	26
4.13	The results of repeating the MACROPA/DEHPA extraction system: 0.005 M MACROPA and 0.001 M DEHPA, back-extraction with 2 M HNO ₃ for 100x diluted Tb/Gd aqueous solution at pH 3.5 as a starting solution, a vortexing time of 10 min and PE 100-140 as the organic phase. Values shown are total EEs after each step.	27
4.14	The results of repeating the MACROPA/DEHPA extraction system: 0.005 M MACROPA and 0.001 M DEHPA, back-extraction with 2 M HNO ₃ for 100x diluted Tb/Gd aqueous solution at pH 3.5 as a starting solution, a vortexing time of 10 min and PE 100-140 as the organic phase. Values shown are EEs for each extraction.	28
4.15	The elution of a clean loading solution (0.05 M HCl) containing 500 mg Gd, 500 μg Tb and 500 μg Dy on the TK212 column. The fraction volume is 40 mL.	29
4.16	The elution of the diluted experiment end product loading solution (0.05 M HCl) containing 500 μg Gd and 4 μg Tb on the TK212 column. The fraction volume is 40 mL.	29
4.17	The UV-Vis spectrum of various compounds, only the MACROPA spectrum differs from the other measured solutions.	30
B.1	The ICP-MS calibration and residual error plots. The calibration at higher ppb is better for both Tb and Gd.	42

List of Tables

1.1	Decay properties of ^{161}Tb and ^{177}Lu . ^{1,6}	1
A.1	Extraction efficiencies [%] of Tb and Gd for various extractants at pH = 1.3. The extractions were carried out with 15 mM Gd and 0.15 mM Tb in HNO_3 as the aqueous phase, PE 100-140 as the organic phase and 10 min vortexing time. The concentrations of the extractants are 0.1 M DEHPA, 0.5 M PC-88A and 0.1 M DDPA with 2 % v/v TBP. The error represents one standard deviation of the mean.	39
A.2	Extraction efficiency [%] of Tb for DEHPA and PC-88A at pH = 1.3 versus extractant concentration. All extractions were carried out with 15 mM Gd and 0.15 mM Tb in HNO_3 as the aqueous phase, PE 100-140 as the organic phase and 10 min vortexing time. The error represents one standard deviation of the mean.	39
A.3	Extraction efficiencies [%] of Tb and Gd for 0.1 M DEHPA and 0.5 M PC-88A versus pH. All extractions were carried out with 15 mM Gd and 0.15 mM Tb in HNO_3 as the aqueous phase, PE 100-140 as the organic phase and 10 min vortexing time. The error represents one standard deviation of the mean.	39
A.4	Extraction efficiencies [%] of Tb and Gd using 0.1 M DEHPA at various pH values. The extractions were carried out with 15 mM Gd and 0.15 mM Tb in HNO_3 as the aqueous phase, PE 100-140 as the organic phase and 10 min vortexing time. The error represents one standard deviation of the mean.	39
A.5	Extraction efficiencies [%] of Tb and Gd using 0.1 M DEHPA and aqueous phase at pH = 1.3. The extractions were carried out with 15 mM Gd and 0.15 mM Tb in HNO_3 , PE 100-140 as the organic phase and various vortexing times. The error represents one standard deviation of the mean.	40
A.6	Extraction efficiency [%] of Tb using 0.1 M DEHPA in chloroform or PE 100-140 with aqueous phase HNO_3 at pH = 1.3. The extractions were carried out with 15 mM Gd and 0.15 mM Tb and 10 minutes vortexing time. The error represents one standard deviation of the mean.	40
A.7	Extraction efficiency [%] of Tb and Gd using 0.1 M DEHPA in PE 100-140 with aqueous phase HNO_3 or HCl at pH = 1.3. The extractions were carried out with 15 mM Gd and 0.15 mM Tb and 10 minutes vortexing time. The error represents one standard deviation of the mean.	40
A.8	The result of a speciation simulation in CHEAQS. The used parameters are: $[\text{Tb}^{3+}] = 0.15 \text{ mM}$, $[\text{Gd}^{3+}] = 15 \text{ mM}$, $[\text{H}^+] = 0.05 \text{ M}$, $[\text{NO}_3^-] = 68.8 \text{ mM}$, 18.8 mM and 68.8 mM, $[\text{Cl}^-] = 28.1 \text{ mM}$, 78.1 mM and 28.1 mM, $[\text{Na}^+] = 0 \text{ M}$, 0 M and 0.5 M and the values given are relative to the initial concentration Gd/Tb added to the solution.	40
A.9	Extraction efficiencies [%] of Tb and Gd. The extractions were carried out with 150 mM Gd and 0.15 mM Tb in HNO_3 as the aqueous phase at pH = 1.3. Various concentrations of DEHPA in PE 100-140 were used as the organic phase and the vials were vortexed for 10 minutes. The error represents one standard deviation of the mean.	40
A.10	BEE [%] of Tb with various concentrations HNO_3 and HCl as the back-extracting agent. The error represents one standard deviation of the mean.	40
A.11	The results of extractions using 0.005 M MACROPA and 0.001 M DEHPA and back-extraction with 2 M HNO_3 for 100x diluted Tb/Gd aqueous solution at pH 2 and pH 3.5, a vortexing time of 10 min and PE 100-140 as the organic phase. The error represents one standard deviation of the mean.	40
A.12	The results of extractions using MACROPA and 0.001 M DEHPA and back-extraction with 2 M HNO_3 for 100x diluted Tb/Gd aqueous solution at pH 3.5, a vortexing time of 10 min and PE 100-140 as the organic phase versus various concentrations of MACROPA. The error represents one standard deviation of the mean.	41

A.13 The results of repeating the MACROPA/DEHPA extraction system: 0.005 M MACROPA and 0.001 M DEHPA, back-extraction with 2 M HNO ₃ for 100x diluted Tb/Gd aqueous solution at pH 3.5 as a starting solution, a vortexing time of 10 min and PE 100-140 as the organic phase. Values given are total EEs after each step.	41
A.14 The results of repeating the MACROPA/DEHPA extraction system: 0.005 M MACROPA and 0.001 M DEHPA, back-extraction with 2 M HNO ₃ for 100x diluted Tb/Gd aqueous solution at pH 3.5 as a starting solution, a vortexing time of 10 min and PE 100-140 as the organic phase. Values shown are EEs for each extraction.	41

Contents

Abstract	i
List of Abbreviations	ii
List of Figures	iv
List of Tables	vi
1 Introduction	1
2 Theory and Background	3
2.1 Nuclear Medicine	3
2.2 Radionuclide Production	4
2.2.1 Production of ¹⁶¹ Tb	5
2.2.2 Separation	5
2.3 Solvent Extraction	5
2.3.1 Lanthanide complexation	7
2.3.2 Terbium complexation	7
2.3.3 Complexation mechanism	8
2.3.4 Separation tuning	8
2.4 Ion Exchange Column Chromatography	9
2.4.1 Columns for lanthanide separation	9
2.5 ICP-MS	10
2.6 UV-Vis spectroscopy	10
2.7 Gamma counting	10
3 Materials and Methods	12
3.1 Equipment	12
3.1.1 Chemicals	12
3.1.2 Disposables	12
3.1.3 Apparatuses	13
3.2 Method	13
3.2.1 Solution preparation	13
3.2.2 Extractions	14
3.2.3 ICP-MS	15
3.2.4 Ion exchange column chromatography	15
3.2.5 UV-Vis measurements	15
4 Results and Discussion	17
4.1 Extractant selection	17
4.2 Extraction optimization	18
4.2.1 pH	18
4.2.2 Vortexing time	20
4.2.3 Organic phase	21
4.2.4 Aqueous phase	22
4.2.5 DEHPA concentration	22
4.3 Back-extraction	23
4.4 MACROPA/DEHPA extraction system	25
4.5 Ion exchange column chromatography	28
4.6 Gadolinium and MACROPA recycling	30
5 Conclusion	31

References	33
A Results	39
B Data Analysis	42
B.1 ICP-MS Data Analysis	42
B.2 Wallac Data Analysis	42

1

Introduction

Radionuclides are widely used in nuclear medicine to either acquire diagnostic information about patients (nuclear imaging) or to treat medical conditions like cancer (nuclear therapy). In the latter, they are injected into the body to target hostile cells directly to weaken or destroy them by damaging their DNA and cell structure through decay radiation.⁷ The number of these medical procedures using radionuclides grows every year, and with it, their demand.⁸ The investigation of their properties and production is therefore an important field of research.

One of the radionuclides currently employed in such therapies is ^{177}Lu , which is used in the treatment of neuroendocrine tumors and prostate cancer. It can be produced in a nuclear reactor, is widely available with high specific activity and chemical purity, and has been broadly studied. Despite the promising studies and treatments, there is always room for further improvement and it is thus important to consider alternative radionuclides with better therapeutic prospects like ^{161}Tb .¹⁻⁶ ^{161}Tb has similar decay properties to ^{177}Lu , see Table 1.1, and also emits low-energy photons that can be used for imaging. It has very similar coordination chemistry meaning it is expected that ^{161}Tb can be used in combination with all the ^{177}Lu -employed chelators like DOTA.^{2,5,6} In contrast to ^{177}Lu however, ^{161}Tb also emits a significant amount of conversion and low-energy Auger electrons. This may raise its therapeutic capability if the nuclide is directly bound to the cell surface or brought close enough to the nucleus of the cell as these electrons have a very short tissue range ($0.5\ \mu\text{m}$) resulting in a high linear energy transfer (LET) ($4 - 26\ \text{keV}/\mu\text{m}$) providing higher local dose densities.^{1,6} Preliminary dosimetry measurements of the use of ^{161}Tb versus ^{177}Lu in the treatment of prostate cancer have shown results favoring the use of ^{161}Tb .⁶ Moreover, Tb has other isotopes that can also be used in nuclear medicine procedures. It has four clinically interesting isotopes which cover all of the nuclear medicine options: ^{152}Tb for positron emission tomography (PET), ^{155}Tb for single-photon emission computed tomography (SPECT), ^{149}Tb for α -decay therapy and finally ^{161}Tb for β^- therapy.^{9,10} All of the above suggests that Tb is a promising radionuclide. It has recently become commercially available with high levels of purity, but upscaling its production is still an ongoing area of research since its demand is expected to keep growing.¹¹

Table 1.1: Decay properties of ^{161}Tb and ^{177}Lu .^{1,6}

Nuclide	Half-life $t_{1/2}$ [d]	Energy emitted beta particles [MeV]	Energy emitted photons [keV]
^{161}Tb	6.906	0.15	74.6 (10.2%); 48.9 (17.0%)
^{177}Lu	6.647	0.14	208.4 (10.4%); 112.9 (6.2%)

^{161}Tb is generally produced through neutron irradiation of ^{160}Gd in a nuclear reactor, but can also be produced in an accelerator where ^{160}Gd is bombarded with a deuteron beam. The production yield in an accelerator is however not competitive with high flux reactors.¹² After neutron irradiation of ^{160}Gd , ^{161}Tb is accumulated via the decay of ^{161}Gd (Eq. 1.1). Up to 4.5 GBq of ^{161}Tb can be theoretically produced after a 2-week irradiation of 1 mg of enriched ^{160}Gd (98.2% purity) at neutron flux of 10^{15} neutrons $\text{cm}^{-2}\text{s}^{-1}$.¹ As current radionuclide therapies of neuroendocrine tumors using ^{177}Lu consist

of four cycles of 7.4 GBq infusions and treatments using ^{161}Tb are expected to be in the same range, the ^{160}Gd targets must be in the range of multiple milligrams to obtain enough ^{161}Tb activity for the treatment of one patient.¹³ To be able to treat more patients both lower-flux irradiation facilities as well as large high-flux facilities must be used or the ^{160}Gd targets must be massive (up to multiple grams).



After irradiation the ^{161}Tb needs to be separated from the ^{160}Gd targets. Since the Gd to ^{161}Tb ratio after irradiation is about 10^3 (neutron flux of 10^{15} neutrons $\text{cm}^{-2}\text{s}^{-1}$) the Gd mass must be reduced significantly to obtain ^{161}Tb with high enough purity.² There are various options concerning the separation of radionuclides and each has its advantages, disadvantages, and application situations. The separation of the two neighboring lanthanides is challenging due to their chemical similarities. The separation of Tb from Gd is even more notoriously difficult as the two are chemically nearly identical; the only notable difference is in their ionic radii (93.5 and 92.3 pm for Gd and Tb respectively).^{14,15} This difference in ionic radii allows for the selective complexation of Gd and Tb by various ligands or chelators. This fact is utilized in their successful separation using ion exchange column chromatography.^{16,17} In a study by Aziz et al., ^{161}Tb was separated from irradiated enriched ^{160}Gd using a cartridge LN resin column after which the final product, $^{161}\text{TbCl}_3$, had a radiochemical and radionuclide purity of $> 99\%$.¹⁸ A combination of TK211/212/221 resins has also been used by Triskem to successfully separate 1 mg μg ^{161}Tb from 1 g of Gd.¹⁷ The problem with this, and other current separation methods, is that they can not handle enough irradiated Gd at a time yet (max. 1 g). Moreover, separation times are quite lengthy (mL/min) and the required columns are large. As mentioned before, scaling up to multiple grams of Gd may be necessary and could allow for irradiation at lower neutron fluxes. To still be able to separate the ^{161}Tb from the Gd successfully by current separation methods, the bulk of the Gd would have to be removed first. This thesis will focus on investigating whether a different extraction method called solvent extraction can be used to remove the bulk of the Gd. The product will then be further purified using ion exchange column chromatography. As enriched Gd is expensive, its recycling possibilities for further irradiation will also be discussed.

This investigation follows a few steps: First a chelator has to be found that is more selective for Tb than Gd to be able to selectively extract Tb from an aqueous solution. The extraction system then has to be optimized for the highest separation by varying the extraction system parameters: extraction pH, chelator concentration, aqueous phase, organic phase, and contact time after which the back-extraction will be studied. In recent years, research has been done on increasing separation in solvent extraction systems by adding a chelator to the aqueous phase to preferentially complex and hold back unwanted co-extractants.^{19,20} This will be investigated for the optimized Tb/Gd extraction system as well. Finally, it will be tested whether the output product of the extraction and subsequent back-extraction can be used in column chromatography for further purification.

First in Chapter 2, some additional background information will be given and the theory surrounding the subject will be discussed. In Chapter 3, the used methods and materials in the project are listed and explained, and in Chapter 4 the results of experiments will be given and discussed. Finally, in Chapter 5 a conclusion will be drawn from the results and recommendations will be made for future research.

2

Theory and Background

This chapter will start by giving some additional background information on radionuclide therapy and the production and separation of radionuclides. Next, solvent extraction will be thoroughly discussed along with the principle of chelation, and some chelator candidates for the separation of Tb from Gd will be presented. Finally, the separation method ion exchange column chromatography is discussed along with the measurement techniques inductively coupled plasma mass spectrometry (ICP-MS), ultraviolet-visible (UV-Vis) spectroscopy, and gamma counting.

2.1. Nuclear Medicine

Nuclear medicine can be split into two main areas: radionuclide therapy and nuclear imaging. In radionuclide therapy the patient is injected with a radiopharmaceutical, the radionuclide, attached to a targeting vector, which delivers radiation to specific locations within the body like tumor sites. The radionuclides then decay and release their radiation damaging the (DNA of the) tumor cells in the process.²¹ The DNA molecule can be damaged in several ways: a break in one strand of the double helix also known as a single-strand break (SSB), a double-strand break (DSB) which is a break in both sides of the double helix, damage to the molecules in between the strands (base damage) and finally, multiple damages to both strands at locations that lie close together (cluster damage).^{21,22} The radionuclides used for these procedures ideally release a high amount of energy in a small volume in and around the tumor and thereby limit the irradiation of surrounding healthy tissue as opposed to external beam therapy where the intermediate tissue is also damaged. The decay characteristics, and with it the possible applications of the radionuclide, vary. The ways a radionuclide can release its energy are visualized in Figure 2.1 and elaborated upon below.²²

α -particles can be released in the decay of heavy nuclides and are helium nuclei. They have a relatively large mass, size, and energy (5 to 9 MeV) compared to the other types of decay radiation and therefore have a higher chance of interaction with other particles. This is why they have the highest ionization power and lowest penetration depth (30 μm). This is quantified in what is called the linear energy transfer (LET) which is the amount of energy per unit distance that an ionizing particle transfers to the material. α -particles have a very high LET (80 $\text{keV } \mu\text{m}^{-1}$). This means that they can produce many ionizations over a short distance possibly leading to many ionizations in one DNA molecule. Because of this, they can do a lot of damage to a single DNA molecule and often cause DSBs which are hard to repair and may lead to the death of the cell.^{21,22}

β -particles come in two forms: β^+ and β^- or positrons and electrons respectively. β^+ decay takes place when there is an excess of protons in the nucleus whereas β^- decay is caused by an excess of neutrons. β -particles have lower energy (0 - 2.3 MeV) and LET (0.2 $\text{keV } \mu\text{m}^{-1}$) than α -particles, but a larger range (up to 12mm). β^- -particles are used in therapy due to their ionizing capabilities, β^+ -particles on the other hand quickly annihilate with an electron and emit 2 photons of 511 keV energy each in opposite directions to preserve momentum. These photons can then be used in diagnostics to locate the site of tumors in an imaging technique called positron emission tomography (PET).

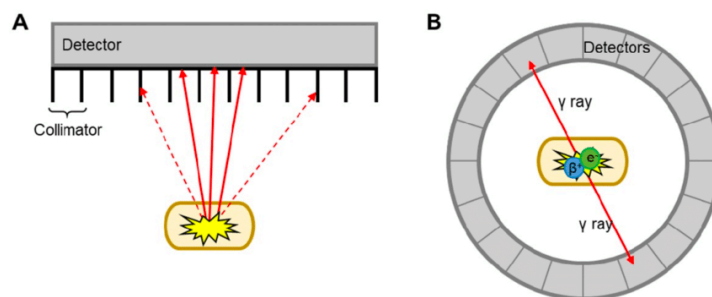


Figure 2.2: A: A visualization of single-photon emission computed tomography (SPECT). A radionuclide emits photons from the site of a tumor that are absorbed by a scintillation crystal and then detected by a gamma camera behind a collimator that only allows the transfer of photons to the camera at right-angles. These rotate so that a 3D image can be made by a computer.

B: A visualization of positron emission tomography (PET). The 511 keV photons resulting from annihilation of an emitted positron with an electron in the body are measured by a ring of detectors and an image is made by a computer.²⁴

When a nucleus has a shortage of neutrons (as opposed to an excess as is the case with α and β^- decay) the nucleus can capture an electron from an inner shell after which a proton transforms into a neutron. This is called electron capture (EC). In internal conversion (IC), the nucleus has excess energy which is transferred to an electron from an inner shell, ejecting it. Both mechanisms lead to an unstable electron cloud and result in the emission of X-ray radiation which can eject electrons from their shell. These ejected electrons are called Auger electrons. Auger electrons have low energy (up to 1 keV) but a high LET (4 to 26 keV μm^{-1}) resulting in many ionizations over a very short range (0.5 μm).

Finally, γ -radiation can be emitted if the nucleus or shell electrons are not in their ground state.

They then shed this excess energy in the form of γ -radiation. The energy of this radiation can be used to determine the type of radionuclide that emitted it. This is because the energy of the emitted photons is nuclide-specific. They can also be used in nuclear imaging procedures like single-photon emission computed tomography (SPECT).

The imaging procedures mentioned above, PET and SPECT, are the two most common in nuclear medicine. They allow for very precise localization of tumor sites.²³ In PET, the 511 keV photons resulting from the annihilation of an emitted positron with an electron in the body are measured by a ring of detectors, Figure 2.2 B. An image can then be made from the simultaneous detection of photons on two opposite detectors as this carries information about the location of the radionuclides in the body and subsequently the location of the tumor. In SPECT, Figure 2.2 A, the radionuclide emits photons from the site of a tumor that are absorbed by a scintillation crystal and then detected by a gamma camera behind a collimator that only allows the transfer of photons to the camera at right-angles. These cameras and collimators rotate so that a 3D image can be made by a computer.²³

2.2. Radionuclide Production

The production of radionuclides can be done in two ways: in accelerators (cyclotrons or linear accelerators) and in reactors. In reactors, the produced isotopes are the result of neutron capture and are therefore neutron-rich whereas the isotopes produced in accelerators are generally proton-rich.

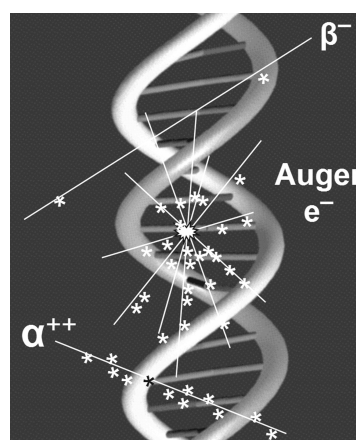


Figure 2.1: A visualization of the types of radiation (α , β and Auger electrons) in radionuclide therapy. The number of ionizations (*) is shown along the path (-) of the decay particles. γ -radiation is not shown.²¹

2.2.1. Production of ^{161}Tb

^{161}Tb is produced from ^{160}Gd in a reactor as discussed in Chapter 1.²⁵ As natural Gd only consists of about 20% ^{160}Gd , an enriched target is required for irradiation because the production of other Tb and Gd isotopes is undesired. An isotope of Gd that may be present is ^{157}Gd (15.65% natural abundance) which is especially undesired as its cross-section is very large compared to ^{160}Gd ($\sigma = 254000$ versus $\sigma = 1.5$). This cross-section negatively influences the neutron flux of the reactor and therefore the reactor power due to self-shielding effects. An enriched Gd target is generally expensive to produce.^{1,26} For designing the separation process this means that it must be kept in mind that the enriched ^{160}Gd target is ideally preserved in such a way that it can be irradiated again. The ^{161}Tb yield when irradiating a highly enriched ^{160}Gd target at 10^{14} neutrons $\text{cm}^{-2}\text{s}^{-1}$ results in a ^{160}Gd to ^{161}Tb ratio of about 10^4 . The Gd must therefore be removed to obtain high purity ^{161}Tb .¹ The ^{161}Tb decays into the stable ^{161}Dy which must also be removed to reach these high purities.

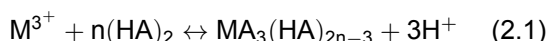
2.2.2. Separation

After production, the daughter radionuclide must be separated from its parent. There are various options concerning this separation and each has its advantages, disadvantages, and application situations: Crystallization, precipitation, or co-precipitation utilizes the solubility difference of compounds in a solution to separate them. Solvent extraction or liquid-liquid extraction (Section 2.3) also utilizes the solubility difference of compounds but in two different phases, an aqueous and an organic phase. (Column) chromatography (Section 2.4) separates based on the different interactions of compounds with two phases, a mobile phase and a stationary phase, as the compounds travel through a supporting medium. Ion exchange column chromatography uses a resin that can exchange bounded ions for ones with selectivity for that resin as the differentiating interaction. Finally, electrolysis uses an external electrical energy source to drive a redox reaction and subsequently separate ions.²⁷

2.3. Solvent Extraction

Liquid-liquid extraction or solvent extraction can be used to separate metals based on a difference in solubility in two immiscible liquids, usually an aqueous and organic phase. As metal ions are usually insoluble in the organic phase, a so-called chelator or ligand is used which is generally highly hydrophobic. The metal and chelator form a complex in a process that is called chelation. It involves the formation of two or more separate coordinate bonds between the chelator/ligand and the central metal atom.²⁸ This is visualized in Figure 2.3.²⁹

In the extraction of rare-earth metals, common extractants are of the organophosphorous kind.³⁰ These are ligands that form complexes with metals through the following reaction:



Here M^{3+} is the metal, HA is the organophosphorous extractant in the organic phase occurring as a dimer $(\text{HA})_2$ and $\text{MA}_3(\text{HA})_{2n-3}$ is the complex formed. The metal is initially dissolved in an aqueous phase and the extractant in the organic phase. When the phases are brought closer together these complexes can be formed.³¹ Following the complex formation and its dissolution in the organic phase, the aqueous and organic phases are separated from each other. The extraction efficiency (EE) of the radionuclide can then be calculated using Equation 2.2 or Equation 2.3 with A the activity of the measured nuclide in Bq. These equations should give the same result if nothing is lost in the extraction procedure.

$$EE\% = A_{org}/A_{total} * 100\% \quad (2.2)$$

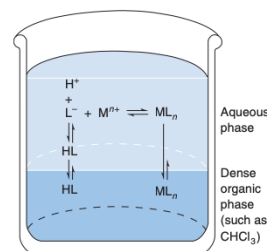


Figure 2.3: A schematic overview of the chelation process. The metal M^{n+} forms a complex ML_n with ligand L which is highly hydrophobic and is therefore extracted to the organic phase.

$$EE\% = \frac{A_{org}}{A_{org} + A_{aq}} * 100\% \quad (2.3)$$

A way in which the separation capability of an extraction system is sometimes quantified is with the separation factor (SF). It is the ratio of the distribution ratios of the metals that are separated and can be calculated with Equations 2.4 and 2.5. Here D_M is the distribution ratio of a metal M, M_{org} and M_{aq} the concentration of the metal in the organic and aqueous phase respectively, and SF the separation factor of two metals.³²

$$D_M = [M_{org}]/[M_{aq}] \quad (2.4)$$

$$SF = D_{M1}/D_{M2} \quad (2.5)$$

The separation of different metals can be achieved by choosing an extractant that is selective for one of them. This metal will then be preferentially extracted which leads to separation. After extraction, the metal ions can be back-extracted from the organic phase by adding a back-extraction agent. This is usually a strongly acidic or basic solution that breaks the bond between chelator and metal. The back-extraction efficiency (BEE) can be calculated using Equation 2.6. The ideal result is a solution containing all the target metal without contaminations from the co-extraction of other metals. The whole process is visualized in Figure 2.4.

$$BEE\% = A_{final}/A_{beforeBE} * 100\% \quad (2.6)$$

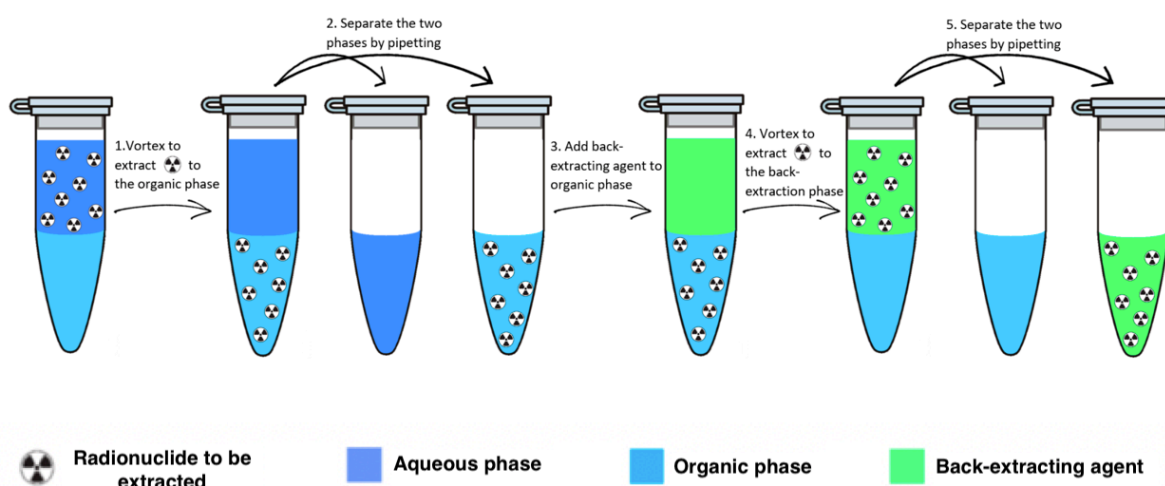


Figure 2.4: A visualization of liquid-liquid extraction and subsequent back-extraction. The vial containing the organic phase with extractant and the aqueous phase with metal is vortexed to allow for faster complex formation. The phases are then separated after which a back-extracting agent is added to the vial with the organic phase to break the complex. Finally, the phases are separated again.

In practice, co-extraction does occur which is unwanted as it contaminates the final solution. Furthermore, the extractant may be slightly miscible in the aqueous solution reducing the achievable extraction efficiency. The selection of chelator and aqueous and organic phases is therefore vital to the success of the extraction.

The solvent extraction approach is constantly developing and novel techniques have been introduced in an attempt to increase extraction efficiencies. One of these is the use of ionic liquids as an organic solvent. They are non-volatile and non-flammable which makes them more environment-friendly than most other organic solvents used in solvent extraction but have high viscosity at room temperature which is not ideal.³³ Successful solvent extraction attempts of lanthanides using ionic liquids have

been reported at an increasing rate in recent years highlighting their potential.^{34–38} Another technique is the use of liquid membranes in a three-phase extraction system consisting of two phases of similar nature but different compositions that are separated by a third phase of different nature, the liquid membrane, that is very insoluble into the other two.³³ In short, the system combines the extraction and back-extraction into a single procedure. The metals diffuse into the organic membrane driven by the difference in pH of the two aqueous phases, form a complex allowing them to move across the membrane and then move into the back-extracting agent where the complex is broken and the metals are back-extracted.³⁹ Research into using this technique in the separation of lanthanides has also been reported.^{40,41}

2.3.1. Lanthanide complexation

Complexes of the lanthanides have very similar chemical properties due to the similarity of the lanthanides themselves. As a result, the selective complexation of lanthanides is not easy. Due to slight differences, like the gradual contraction of the ionic radii across the series, the stability constants of the lanthanide complexes do differ slightly. There are three possible trends in these stabilities:¹⁵

1. In most cases the stability constants increase steadily across the lanthanide series
2. Some ligands form complexes whose stability increases along the first part of the series before reaching a maximum and then remaining constant or even decreasing for the late lanthanides.
3. Very few ligands form complexes with decreasing stability across the series⁴²

The first trend is caused by the fact that ligands can form complexes with lanthanides based on their electrostatic interaction. The decreasing ionic radius and subsequent increasing charge density across the series allows for increasing complex stabilities for the heavier lanthanides. The second trend is not of interest to this thesis as the stability constants for the middle lanthanides Tb and Gd are too similar here by definition of the trend. The last trend applies to complexes with higher steric restrictions, they are better suited for the coordination of lanthanides with higher ionic or atomic radii.¹⁵

Because Tb and Gd are so similar, finding an extractant that is selective for Tb is very difficult. Again, the only real difference between the two is in their ionic radii; Tb has a slightly smaller one than Gd (92.3 vs 93.5 pm).¹⁵ This results in a higher surface charge density for Tb which makes it more susceptible to complexation with ligands that form complexes through electrostatic interactions. As ligands exhibiting reverse-size selectivity for lanthanides are rare, it is therefore proposed to look for a chelator that can extract more of the Tb than the Gd and optimize its separation behaviour. Synergistic complexation can also be investigated. This is the process of using two or more ligands in a single extraction to potentially raise the entropy of the configuration and to subsequently enhance extraction.⁴³

2.3.2. Terbium complexation

Solvent extraction of rare-earth metals (REEs) from phosphoric acid solutions was investigated by Sato et al.^{44,45} Here, di-(2-ethylhexyl)-phosphoric acid (DEHPA/HDEHP) and 2-ethylhexylphosphonic acid (EHEHPA/HEHEHP/PC-88A) in kerosene were used to extract the metals. The extraction efficiencies of Tb, Gd, and Dy showed differences but were very similar, again showing the challenge concerning their separation. The extraction with DEHPA was also studied by Innocenzi et al. where the EE was again better for Tb than Gd, especially at lower pH.⁴⁶ DEHPA has also been used in combination with tributyl-phosphate (TBP) to extract Gd, Tb, and Dy from nitrate media.^{47,48}

Extraction of Tb and Dy was attempted by using PC-88A as a ligand and kerosene as an organic phase by Kurihara et al.⁴⁹ It was found that Dy was extracted more than Tb as again heavier REEs are generally extracted more than lighter ones. More than 90% of both metals could be extracted from the aqueous solution. PC-88A was also used to extract Tb from phosphoric acid solutions by Radhika et al. where a 90% EE was observed as well.⁵⁰

An attempt to separate Tb from Gd using solvent extraction was done by Chiola et al. where dodecylphosphonic acid (DDPA) was used as an extraction agent and TBP was used to achieve good phase separation with kerosene as the organic phase. The EE of Tb was slightly lower than 60% and the EE of Gd was 20% in the best case, thus showing good separation.⁵¹

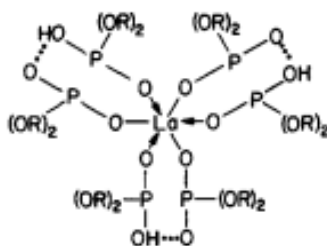


Figure 2.5: The DEHPA-lanthanide complex, DEHPA forms the complex as a dimer according to Equation 2.2.⁶¹

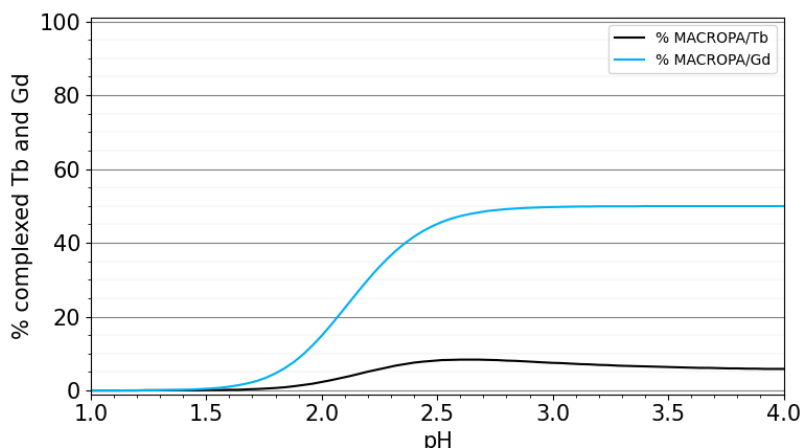


Figure 2.6: The amount of complexed Tb and Gd ($[Gd] = 15 \text{ mM}$ and $[Tb] = 0.15 \text{ mM}$) with 0.5 M MACROPA versus pH, as calculated by HYSS using the stability constants of MACROPA-lanthanide complexes as reported by Roca-Sabio et al.⁶²

The solvent extraction of rare earths from aqueous solutions is also discussed by Xie et al.⁵² Here, DEHPA and PC-88A are mentioned as the most widely used extractants to extract the rare earths.

Other extractants that have been reported to be able to extract Tb (and Gd) from aqueous solutions include Cyanex 272 and Cyanex 572.^{53–59} These were not available to us and will therefore not be used in this thesis.

2.3.3. Complexation mechanism

DEHPA, PC-88A, and DDPA in combination with TBP are therefore all viable options for the separation due to their (slight) selectivity for the heavier lanthanides and/or because they can extract most of the Tb from an aqueous solution at a certain pH which is desired. TBP is a solvating extractant that can assist in extractions by replacing other ligands in the complex formation.⁶⁰ The other three ligands are all organophosphorous ligands that form complexes through the reaction in Equation 2.2. A visualization of the formed complex by DEHPA with a lanthanide is shown in Figure 2.5. It can be seen that DEHPA forms the complex as a dimer. Other complex structures where only one or two Cl^- or NO_3^- group(s) is/are replaced by a DEHPA dimer are also possible. This phenomenon is less likely for the Cl^- group however as the lanthanide is more likely to occur in its free form in a chloride medium.⁶¹ The separation of Tb and Gd using solvent extraction by complexation with organophosphorous ligands will be further investigated in Chapter 4.

2.3.4. Separation tuning

As mentioned in the introduction, in recent years there has been research towards increasing separation in solvent extraction systems by adding a chelator to the aqueous phase to preferentially complex and hold back unwanted co-extractants.^{19,20,63–65} Reverse size selective aqueous chelators for the

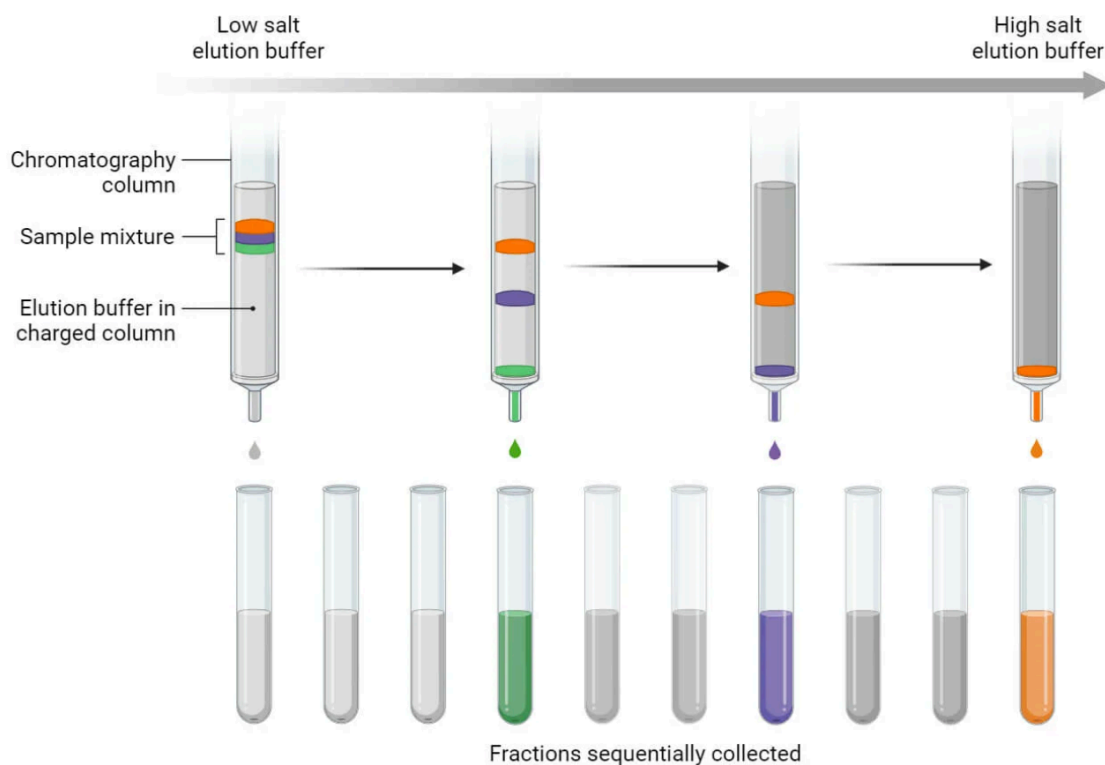


Figure 2.7: The ion exchange column chromatography process, first the sample mixture is loaded onto the column replacing the ions initially bounded. The column is then sequentially eluted with an increasingly higher salt elution buffer and the fractions are collected. The ions will come out of the columns in order of the strength with which they are bounded, from low to high resulting in their separation.⁶⁸

lanthanides are rare but do exist. One of these is MACROPA which is a chelator that has shown unprecedented selectivity for lanthanides, even Tb and Gd.^{42,62} To show this, a speciation diagram was made with a program called HYSS (Hyperquad Simulation and Speciation)^{66,67} using the stability constants of MACROPA-lanthanide complexes as reported by Roca-Sabio et al. and is shown in Figure 2.6.⁶² The concentrations used are 15 mM Gd, 0.15 mM Tb, and 0.5 M MACROPA. It can be observed that at high enough pH, half of the Gd has formed a complex while only 5% of Tb has. These complexes are not extracted to the organic phase by an extractant. This principle of separation tuning using a reverse size selective chelator to enhance separation will be further investigated in Chapter 4.

2.4. Ion Exchange Column Chromatography

Ion exchange column chromatography is a process that separates ions and polar molecules based on their relative interaction with an inert matrix in a column.⁶⁸ When separating lanthanides a cationic exchange matrix or resin is used that usually consists of different mixtures of organophosphoric, organophosphonic, and organophosphinic acids in an insoluble phase.¹⁷ The sample mixture is then loaded onto the column replacing the ions initially bounded. The ions in the loaded mixture have a different affinity to bind to the matrix and will therefore spread out accordingly. The column is then sequentially eluted with an increasingly higher salt elution buffer and the fractions are collected. The ions will come out of the columns in order of the strength with which they are bounded, from low to high. In doing this, the ions present before loading replace the eluted ones again, regenerating the matrix. This process is visualized in Figure 2.7.⁶⁸

2.4.1. Columns for lanthanide separation

The columns used for the separation of lanthanides typically use a cationic exchange matrix or resin that consists of different mixtures of organophosphoric, organophosphonic, and organophosphinic acids in an insoluble phase. The TK211 and TK212 resin columns developed by Triskem also use such a matrix.

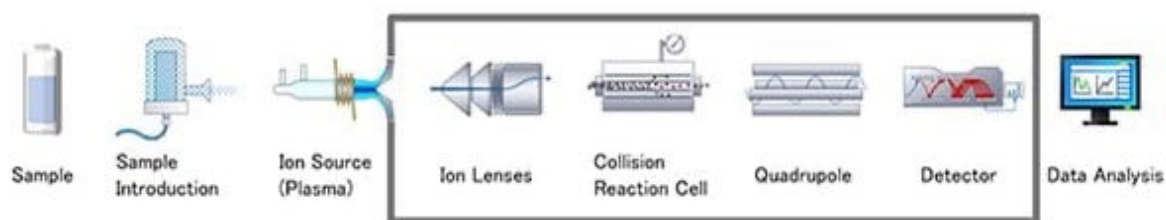


Figure 2.8: An overview of the ICP-MS system.⁷⁰

They have shown that a sequential use of their TK212 and TK211 columns can separate 1 mg Tb from 1 g Gd and 1 mg Dy. These columns are very large, 150 mL for the TK211 and 53 ml for the TK212 column and can be eluted at max. 15 mL/min which limits the separation speed.^{17,69} This indicates the need for a pre-column bulk separation method. The TK212 column is used in Chapter 4 to show its separation capabilities after using the developed separation method in this thesis.

2.5. ICP-MS

Inductively coupled plasma mass spectrometry is a very powerful technique that enables the detection of elements in a solution with parts per billion (ppb) precision. It is used to measure liquid samples. These samples are first pumped into a nebulizer where they are converted into an aerosol mist using a jet of argon gas. The larger droplets are then removed and the rest are carried to the ICP plasma torch where the plasma is formed by transferring energy to the argon gas via inductive coupling from a load coil wrapped around the outside of the tube the gas flows through. The free electrons in the argon gas obtain enough energy to ionize the argon atoms starting a cascade of ionization which finally results in a plasma. The ions in the plasma are then transferred to the mass spectrometer through a vacuum interface and focused into a narrow beam by an ion lens. This lens also separates the ions from the neutral photons and neutrons that are still present. Next, the ions enter a collision/reaction chamber (CRC) that is usually pressurized with helium. The helium slows down the ions, the polyatomic ones more than the analyte ones, allowing for the discrimination between the two in a process called kinetic energy discrimination (KED) where only the higher kinetic energy analyte ions are selected. Now the ions enter a mass filter where they are filtered by mass to charge ratio so only the elements to be measured are measured. These ions strike a dynode, releasing one or more electrons that strike another dynode, releasing more electrons, and so on. This signal is then measured by the electronics. For data processing, the system is calibrated by measuring samples with known concentrations. Usually several of these reference samples are measured to create a calibration plot of counts versus known concentration for each element. An overview of the process can be found in Figure 2.8.⁷⁰

2.6. UV-Vis spectroscopy

UV-Vis spectroscopy is an analytical measurement technique that measures the amount of UV and visible light that is absorbed (or transmitted) by a sample in comparison to a reference or blank sample. It can do this at specific wavelengths by using a monochromator for quantitative measurements or at a range of wavelengths for more qualitative results. Quartz sample holders are required for measurements in the UV range since plastic and glass absorb most of the UV light and quartz does not. After passing through the sample, the non-absorbed light hits a detector that converts it to an electronic signal. The absorbance is then calculated using Equation 2.7 where A is the absorbance $[-]$, I_0 $[W/m^2]$ is the intensity of light before passing through the sample and I $[W/m^2]$ is the intensity after passing through the sample.⁷¹

$$A = \log_{10}(I_0/I) \quad (2.7)$$

2.7. Gamma counting

Gamma counting can be done with a thallium-activated sodium iodide detector (NaI(Tl) detector). It consists of a NaI(Tl) crystal, a photomultiplier tube, and a multichannel analyzer. The incoming gamma

rays interact with the crystal, are absorbed, and produce light within the crystal. This light hits a photocathode and produces an electron that is multiplied by a series of dynodes. The resulting electrons then hit an anode and the multichannel analyzer converts the overall obtained pulse into a digital signal. The energy of the incident gamma ray corresponds to the height of the resulting electron pulse which allows for the production of a spectrum.²²

3

Materials and Methods

3.1. Equipment

Below the used chemicals, disposables, and apparatuses are listed with their production company and model information.

3.1.1. Chemicals

Inorganics

	Manufacturer
• Tb ₄ O ₇	Sigma-Aldrich
• TbCl ₃	Acros Organics
• Tb(NO ₃) ₃ · 6H ₂ O (99.9% purity)	Aldrich
• Gd(NO ₃) ₃ · 6H ₂ O (99.9% purity)	Aldrich
• Dy(NO ₃) ₃ · 5H ₂ O (99.9% purity)	Aldrich
• HNO ₃ (69 wt%)	Honeywell
• HCl (30 wt%)	Supelco
• NaOH	Honeywell
• Tb ICP standard solution (1000 ppm)	VWR (Avantor) International BV
• Gd ICP standard solution (1000 ppm)	VWR (Avantor) International BV
• MilliQ water (18.2 MΩ)	-
• MACROPA	University of Coruña

Organics

	Manufacturer
• Petroleum benzene boiling range 100-140 °C	Emplura
• Chloroform	Sigma-Aldrich
• Benzene	Fluka
• Di-(2-ethylhexyl)-phosphoric acid (DEHPA)	Sigma-Aldrich
• 2-ethylhexylphosphonic acid (PC-88A)	TCI Europe
• Tributyl-phosphate (TBP)	Sigma-Aldrich
• Dodecyl-phosphonic acid (DDPA)	TCI Europe

3.1.2. Disposables

	Manufacturer
• 1.5, 5, 15 and 50 mL vials with screw cap	Sarstedt
• Pipettes	Biohit
• Pipette tips	Biohit
• Universal Indicator Paper pH 1-14	-
• TK212 resin column	Triskem
• Peek tubing	-
• 1.5 mL UV-cuvettes	VWR

3.1.3. Apparatuses

	Manufacturer
• ICP-MS	Perkin Elmer - NexION [®] 2000
• Vortex machine	Scientific Industries - Vortex Genie 2
• Balance	Mettler Toledo - AE240
• Gamma Counter	Perkin Elmer - 2480 Automatic Gamma Counter Wizard ² 3" (Wallac)
• pH meter	Metrohm - 774
• HPLC gradient pump	Shimadzu - LC 10AI
• Fraction collector & auto-sampler	Lambda Omnicoll
• UV-6300PC Double Beam Spectrometer	VWR

3.2. Method

3.2.1. Solution preparation

¹⁶⁰Tb stock solution

To prepare the ¹⁶⁰Tb stock solution, 7 mg of Tb₄O₇ was irradiated by neutrons at thermal flux of 5×10^{12} [W/m²] for 10 hours at the BP3 irradiation facility in the Hoger Onderwijs Reactor (HOR) after which the final product had an activity of 7.59 MBq on October 24 2023. This was dissolved in 0.5 mL concentrated HCl (9.71 M) and 0.5 mL concentrated HNO₃ (15.6 M) by leaving it in an ultrasonic bath at 60°C for 1 hour.

Non-radioactive Tb stock solution

To prepare the non-radioactive Tb stock solution 10 mg of TbCl₃ was dissolved in 1 mL MilliQ water.

Aqueous solutions - Wallac measurements

To make aqueous solutions containing $1.5 \cdot 10^{-2}$ M or $1.5 \cdot 10^{-1}$ M Gd³⁺ and $1.5 \cdot 10^{-4}$ M Tb³⁺ in HNO₃ or HCl, 13.75 or 137.5 mg Gd(NO₃)₃ · 6H₂O was added to a vial containing 2 mL HNO_{3, aq} or HCl_{aq} with certain pH and stirred until dissolved. 2 μL of the ¹⁶⁰Tb stock solution was added to 0.5 mL of the solution. Since this solution contained very concentrated acids this lowered the pH significantly. To obtain solutions with pH 1.5 and higher, 0.1 and 1 M NaOH_{aq} were added to the initial 2 mL solution to obtain the correct final pH. The amount of Gd(NO₃)₃ · 6H₂O that was added was scaled accordingly to maintain its concentration.

Aqueous solutions - ICP measurements

To make solutions containing non-radioactive Tb for ICP-MS measurements, the non-radioactive Tb stock solution was used instead of the ¹⁶⁰Tb stock solution.

Aqueous solutions - MACROPA

To make aqueous solutions containing the chelator MACROPA, the solution without activity was diluted 100 times. MACROPA was added to make 0.0001, 0.001, 0.005 and 0.01 M MACROPA solutions.

Organic solutions

To make organic solutions containing various concentrations of a chelator the chelators were dissolved in either PE 100-140, benzene, or chloroform at final concentrations 0.001 M - 1.0 M. DEHPA and PC-88A are liquid chelators, they were added to a vial which was then filled with solvent. DDPA was added in combination with 2 % v/v TBP as TBP serves as a modifier to achieve good phase separation and its presence is shown to improve the separation between Gd and Tb if used with DDPA.⁵¹ In making the DDPA/TBP solution, not all DDPA dissolved which resulted in a cloudy solution with some DDPA left at the bottom of the vial (see Figure 3.1).



Figure 3.1: The DDPA/TBP solution. Not all DDPA has dissolved resulting in a cloudy solution with the undissolved DDPA powder at the bottom of the vial.

3.2.2. Extractions

To determine the Tb EE of a solvent extraction experiment the Tb activity was measured on the Wallac gamma counter. The Gd EE was determined by concentration measurements on the ICP-MS as explained in appendix B.1. For measuring the Gd EE all experiments were repeated with the non-radioactive aqueous solution. Here, samples were taken of the aqueous phase before adding the organic phase and after extraction, diluted according to Section 3.2.3 and then measured on the ICP-MS. For the Tb activity measurements, vials were weighed before and during the experiments to be able to correct for volume as discussed in appendix B.2. The data of both the Wallac and ICP-MS was processed as described in appendix B.

Chelator selection

To select a good chelator for the separation of Tb from Gd, 0.5 mL of organic solution containing 0.1 M DEHPA, 0.5 M PC-88A, or 0.1 M DDDPA with 2 % v/v TBP in PE 100-140 was added to 0.5 mL of aqueous solution containing Tb and Gd at pH 1.3. The Tb activity of these vials was measured beforehand on the Wallac. After adding the organic phase the vials were vortexed for 10 minutes. 0.3 mL of the organic phase was pipetted into another 1.5 mL vial. The same was done with the aqueous phase after which all vials were measured again on the Wallac. For a second experiment, the first experiment was repeated for organic solutions containing 0.1 M DEHPA and 0.5 M PC-88A in PE 100-140 but now with an aqueous solution containing Tb and Gd at pH 1.1 and 1.2. For a third experiment, the first experiment was repeated but now with organic solutions DEHPA or PC-88A in PE 100-140 at concentrations 0.05, 0.1, and 0.5 M.

Extraction optimization

To optimize the extraction of Tb and its separation from Gd using DEHPA the system was optimized for several parameters. Apart from the to-be-optimized parameter, the procedure was equal to the one followed in the first chelator selection experiment using 0.1 M DEHPA in PE 100-140, HNO₃ containing Tb and Gd, a pH of 1.3 and 10 min vortexing time. To determine the influence of the pH it was varied from 0 to 5. The influence of the vortexing time was determined by varying it from 30 seconds to 10 minutes. PE 100-140, chloroform, and benzene were tested as organic phase. HNO₃ and HCl as aqueous phase. To determine whether increasing the Gd/Tb ratio affects the separation, a higher concentration of Gd and various DEHPA concentrations were used.

Back-extraction

To optimize the back-extraction the activity of the organic phase after an experiment was measured on the Wallac. An equal volume of HNO_{3, aq} or HCl_{aq} (1.0, 1.5, 2.0, 3.0, 4.0 or 5.0 M) was added and the vial was vortexed for 10 min. The phases were then separated and their activity was measured on the Wallac to determine the BEE of Tb with Equation 2.6. The BEE of Gd was determined by comparing its concentration in the aqueous phase after extraction to its concentration in the back-extracting agent after back-extraction. The validity of the BEE of Gd therefore relies on the assumption that no Gd was lost in the extraction procedure.

MACROPA

The optimized DEHPA extraction was used in combination with MACROPA in the aqueous phase to increase the separation. To optimize the combined system, the MACROPA concentration and the pH were varied. The extraction was followed by a back-extraction with 2 M HNO₃. The EEs were determined by taking a sample of the aqueous phase before adding the MACROPA and comparing it to a sample of the back-extracting agent after back-extraction. These samples were diluted as described in Section 3.2.3 and then measured on the ICP-MS.

Sequential extractions

Finally, sequential extractions were performed by employing the same procedure as in the MACROPA-DEHPA experiment with 0.005 M MACROPA and a pH of 3.5. After each extraction and subsequent back-extraction, the pH of the final solution (2 M HNO₃ containing the extracted Tb and Gd) was adjusted by adding 1 M and 0.1 M NaOH until it reached a value between 3 and 4. This is difficult since the back-extracting agent is highly acidic so aqueous and organic phase volumes of 5 mL were used for these experiments. The extraction was performed again after raising the pH by adding an equal

volume of organic phase. This was then repeated once more. Samples of the back-extracting agent were taken before and after each extraction and subsequent back-extraction to determine the EE of each step.

3.2.3. ICP-MS

For measurements on the ICP-MS, taken samples were diluted with 1% v/v HNO₃. The dilution factor depended on the expected Gd concentration in the sample as the measured Gd concentration on the ICP can not exceed 500 ppb to ensure minimal degradation of the measurement device.

3.2.4. Ion exchange column chromatography

The column used to separate Tb and Gd was the TK212 resin column developed by Triskem. Two separation experiments were done, one with a 'clean' loading solution and one with a diluted end product of an extraction and subsequent back-extraction using the MACROPA/DEHPA system. To prepare the 'clean' loading solution, 1435, 0.14 and 0.14 mg of Gd(NO₃)₃ · 6H₂O, Tb(NO₃)₃ · 6H₂O and Dy(NO₃)₃ · 5H₂O respectively was dissolved in 300 mL 0.05 M HCl. To prepare the experiment loading solution, the MACROPA/DEHPA extraction was done as described in Section 3.2.2. The back-extraction was done with 2 M HCl instead of HNO₃. The back-extracted solution was diluted 40x to get a 0.05 M HCl solution. This was added to 0.05 M HCl until the final volume was 300 mL as required for loading. In Figure 3.2, the setup for the ion exchange column chromatography experiments is shown. The column was preconditioned with 0.05 M HCl by slowly increasing the flow rate (e.g. rinse at 3 mL/min for a couple of minutes, then 5 mL/min, etc. until the flow rate was reached that was used during the separation: 9.99 ml/min. It was then loaded with the 300 mL loading solution after which the column was first eluted with 1360 mL 0.2 M HNO₃ and then 1360 mL 0.5 M HNO₃. 72, 40 mL fractions were collected in 50 mL vials; 4 from the final 160 mL loading phase and 2x 34 from the elutions. These fractions were diluted and measured on the ICP-MS.

3.2.5. UV-Vis measurements

1 mL of the end product of a MACROPA/DEHPA extraction as described in Section 3.2.2 but back-extracted with 2 M HCl, 1 mL 0.001 M DEHPA in PE-100-140, 1 mL 0.005 M MACROPA in 2 M HCl and a 1 mL 2 M HCl, $1.5 \cdot 10^{-2}$ M Gd³⁺ and $1.5 \cdot 10^{-4}$ M Tb³⁺ solution were added to UV-cuvettes and measured on the UV-spectrometer in the 230-900 nm range with steps of 1 nm. A 1 mL 2 M HCl solution was used as a reference.



Figure 3.2: 1: Loading/elution solution, 2: Tubing, 3: Pump, 4: Purge tube for removing air, 5: Column inlet, 6: Column, 7: Column outlet, 8a: Tubing to waste container, 8b: Tubing to vials, 9: Fraction collector, 10: Collection vials.

4

Results and Discussion

In this chapter, the results of the experiments as described in Chapter 3 are presented and discussed. All experiments are carried out in triplicate and the reported associated error or the size of the error bar corresponds to one standard deviation of the mean. Results are tabulated in the Appendix (A).

The ratio of Gd versus Tb in the solutions is kept at 100 throughout all experiments unless mentioned otherwise. This is to approach the 10^4 ratio that would be the result after irradiation of Gd. This 10^4 ratio is not used for various reasons: First, the amount of Tb that can be minimally used is fixed when measuring on the Wallac due to the limited amount of activity that is present. The same goes for measuring on the ICP-MS as there the Tb is already at the lower (and the Gd at the upper) limit of detection. Finally, the amount of Gd that can be maximally used is also limited due to its availability. The ratio is increased in one experiment to show increasing it does not result in substantial decrease in separation.

Since the Tb EE is calculated with Equation 2.3 and the Gd EE with Equation 2.2 due to differing measurement techniques, comparison between the two relies on a similar result of the equations. This is expected when there are no losses in the extraction, i.e. the combined amount in the aqueous and organic phase equals the total amount. If there are losses, Equation 2.3 yields results that are too high. However, no loss of Tb was measured and comparison is therefore possible.

4.1. Extractant selection

For selecting an extractant with the best separation potential for Tb and Gd various experiments were performed. The EEs of Tb and Gd for three extractants are shown in Figure 4.1. The pH for the extraction was difficult to select as data in literature for solvent extraction of lanthanides is hard to compare due to a high variety in ionic strength and type of aqueous media, used organic phases, and concentration of extractant.⁴⁸ Most literature concerning the separation of Tb, Gd, and Dy uses pH values between 0 and 2, however, since a higher EE was reported at a higher pH, the highest pH that could be made without having to adjust the ionic strength was used.^{44,46–51} In Figure 4.1, the DDPA/TBP combination showed the best selectivity for Tb (73.6 ± 2.5 % Tb EE vs 47.8 ± 1.5 % Gd EE) while DEHPA and PC-88A were able to extract the most Tb, EEs of 98.3 ± 0.5 % and 98.6 ± 0.2 % respectively. The lower EE for DDPA/TBP at this pH could be explained by its lower concentration compared to the other two extractants as it did not fully dissolve or because the pH of the aqueous phase was too low. Raising the pH can improve the EE as will be discussed in Section 4.2. In any case, the lower dissolution and therefore concentration of extractant in the organic phase is undesired as it limits the amount of metal that can be extracted. DDPA was therefore discarded as an extractant option.

To investigate the extraction differences between DEHPA and PC-88A the EEs of Tb were investigated at other extractant concentrations and EEs of Tb and Gd at varying pH values. The results of these experiments are shown in Figure 4.2. Near 100 % Tb EE can be achieved with both extractants, but DEHPA does this at lower concentrations. EEs of Gd with DEHPA are lower in the measured pH range. Lowering the PC-88A concentration could result in a lower Gd EE but this would also result in a lower

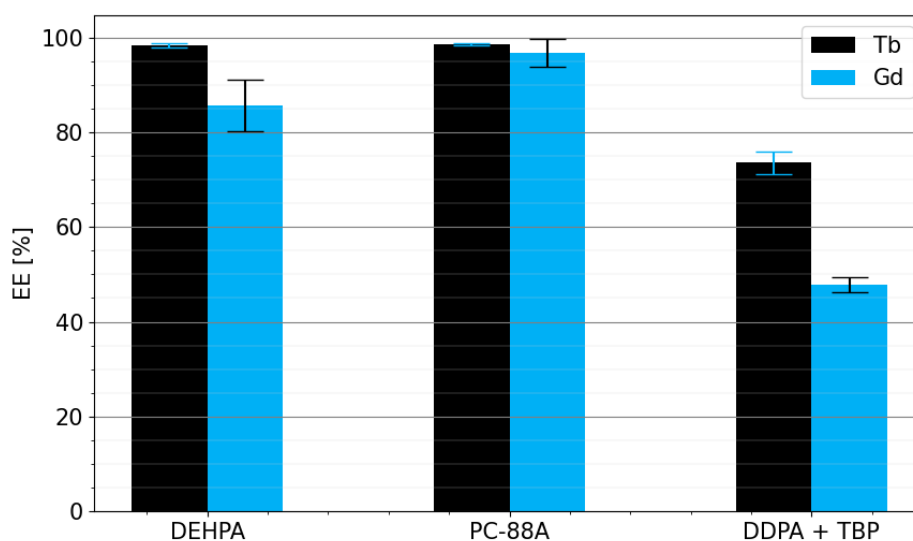


Figure 4.1: Extraction efficiencies [%] of Tb and Gd for various extractants at pH = 1.3. The extractions were carried out with 15 mM Gd and 0.15 mM Tb in HNO_3 as the aqueous phase, PE 100-140 as the organic phase and 10 min vortexing time. The concentrations of the extractants are 0.1 M DEHPA, 0.5 M PC-88A and 0.1 M DDPA with 2 % v/v TBP. The error bars represent one standard deviation of the mean.

Tb EE which is undesired. DEHPA is therefore selected as an extractant. The extraction using DEHPA will be optimized to improve separation, i.e. extract less Gd whilst still extracting near 100 % Tb. The results of this optimization are reported in the following section.

4.2. Extraction optimization

To optimize the DEHPA extraction system multiple parameters can be varied. These include the pH of the aqueous phase, the vortexing time, the type of organic phase, the type of aqueous phase and the DEHPA concentration. The results of this optimization will now be discussed.

4.2.1. pH

In Figure 4.3, the results of the extraction are shown for a wide range of pH values. The EE of both Tb and Gd increases with pH. This is caused by the protonation of DEHPA at lower pH values (or deprotonation at higher pH values). The higher the concentration of H^+ atoms in the solution, the less free DEHPA and the lower the EE. Furthermore, the amount of free DEHPA that is dissolved in the aqueous phase grows with pH facilitating the complex formation and subsequent extraction.^{72,73} This pH dependence in solvent extraction of lanthanides by DEHPA is heavily supported by literature.^{30,48,74–78} In Figure 4.3, it can also be observed that at pH 1.5 and higher, the EEs drop slightly. This is an unexpected result as all of the above suggests an increase in EE with pH up to the maximum EE of the system. There are however a few differences in extraction conditions other than pH that can be the cause of this discrepancy.

First, the pH of aqueous solutions with pH 1.5 and higher containing radioactive Tb was raised using various amounts of NaOH as discussed in Section 3.2.1. This addition of Na^+ ions to the aqueous phase raises its ionic strength. A higher ionic strength is reported to have a positive effect on the EE in solvent extraction due to the 'salting-out effect'.^{34,79,80} Salting out is the phenomenon observed when the solubility of a compound in an aqueous phase decreases with an increase in the concentration of a salt. In this case, adding more Na^+ ions could mean a decrease in solubility of Tb and Gd, pushing them towards the organic phase, facilitating the complex formation with DEHPA, and subsequently increasing the EE. This is however not what is observed, as the EE is lower.

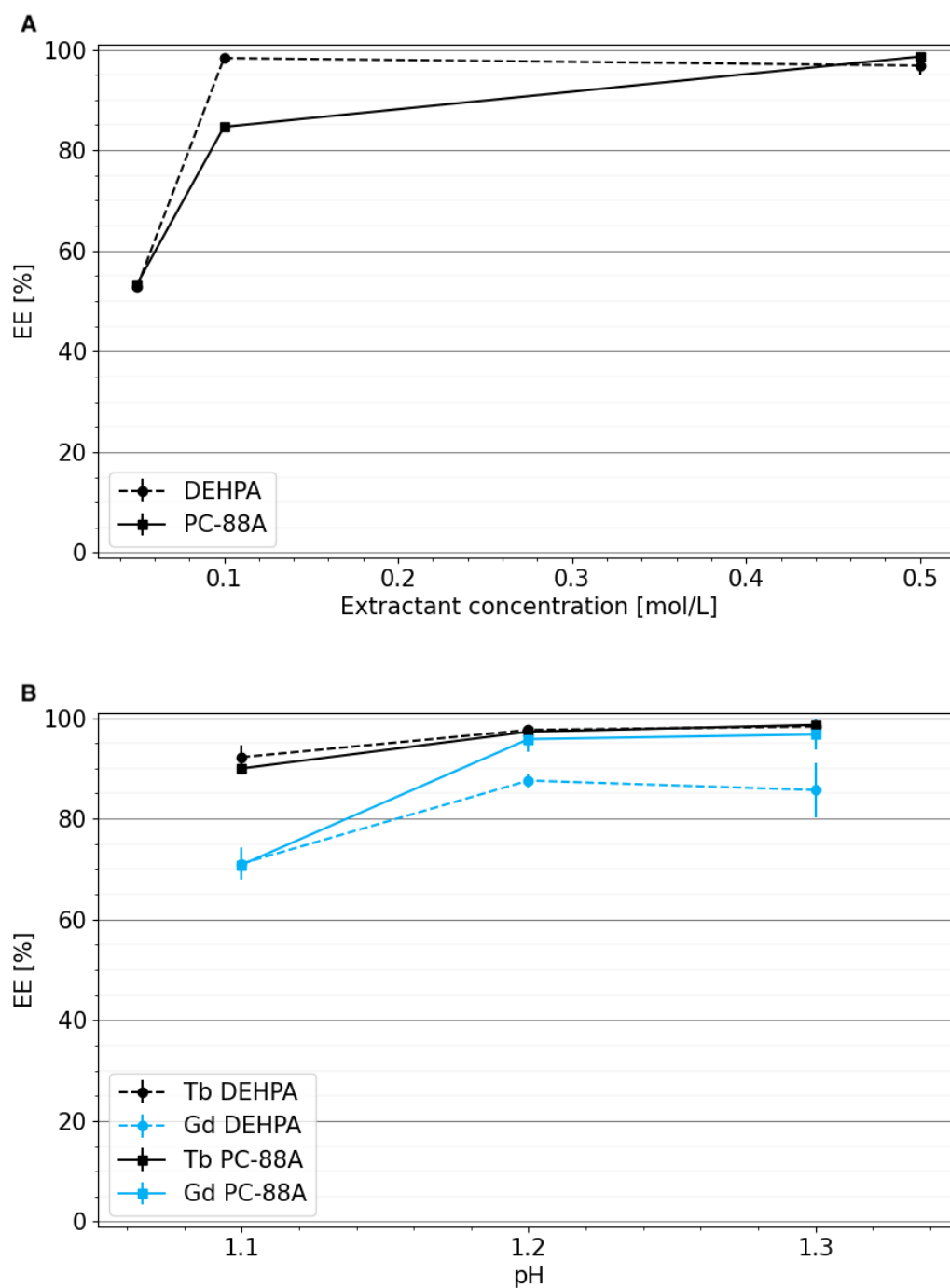


Figure 4.2: A: Extraction efficiency [%] of Tb for DEHPA and PC-88A at pH = 1.3 versus extractant concentration. Bottom: Extraction efficiencies [%] of Tb and Gd for 0.1 M DEHPA and 0.5 M PC-88A versus pH. All extractions were carried out with 15 mM Gd and 0.15 mM Tb in HNO_3 as the aqueous phase, PE 100-140 as the organic phase and 10 min vortexing time. The error bars represent one standard deviation of the mean.

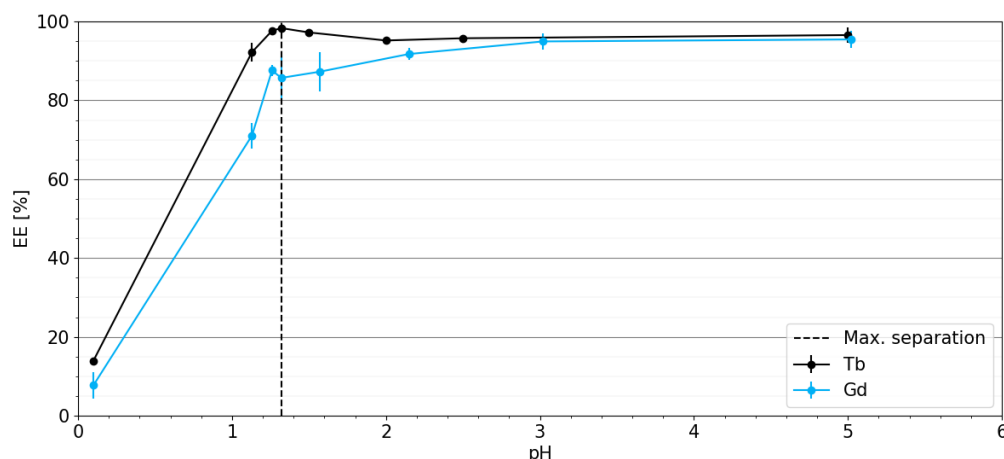


Figure 4.3: Extraction efficiencies [%] of Tb and Gd using 0.1 M DEHPA at various pH values. The extractions were carried out with 15 mM Gd and 0.15 mM Tb in HNO_3 as the aqueous phase, PE 100-140 as the organic phase and 10 min vortexing time. The error bars represent one standard deviation of the mean. The lines serve to guide the eyes but have no scientific meaning.

A second possibility is that the co-extraction of Na^+ ions decreases the EE of Tb and Gd. This was however not seen by Devi et al. and Shibata et al. in the extraction of Co^{2+} with sodium salts of DEHPA and is therefore not expected here either.^{59,81}

A third option is that the Na^+ ions bind with the NO_3^- ions reducing the amount of GdNO_3^{2+} and TbNO_3^{2+} in the solution. This means that relatively more DEHPA is needed for the extraction as discussed in Sections 2.3.3 and 4.2.4, lowering the EE. This was confirmed by a speciation simulation in CHEAQS (Table A.8): an increase in Na_{aq}^+ ions leads to a decrease in the concentration of GdNO_3^{2+} and TbNO_3^{2+} . An experiment at pH = 3.5 with 100 times less Tb, Gd, and DEHPA measured on the ICP-MS without using NaOH to raise the pH resulted in EEs of both Tb and Gd of 100.0 ± 0.0 % suggesting that the additional $\text{Na}^+(\text{aq})$ ions could have had a negative effect on the EE.

Finally, the temperature differed between the lower and higher pH experiments. The lower pH experiments were done in November at $\pm 20^\circ\text{C}$ and the higher ones in January at $\pm 18^\circ\text{C}$. It is reported that a lower temperature can decrease the EE as it decreases mass transfer between phases and can decrease the solubility of compounds in solutions.⁸²⁻⁸⁶ However, the reverse is also reported indicating that this influence is very system-specific.⁸⁷⁻⁹¹ More investigation is therefore required into the temperature dependence of the extraction system used here. It should be noted that all other experiments were performed at least within a period of a few days from each other at very similar lab temperatures. The potential temperature influence is therefore assumed to be absent there. The maximum separation at high Tb EE was at pH = 1.3 (98.3 ± 0.5 % Tb versus 85.7 ± 5.5 % Gd), the subsequent experiments were therefore performed at that pH.

4.2.2. Vortexing time

Extractions were carried out at a range of vortexing times to determine its influence on the EE. The results are shown in Figure 4.4. The extraction is very fast, after 30 seconds most of the Tb and Gd has formed a complex and moved to the organic phase. The same is observed by Kumari et al. in the extraction of other lanthanides with DEHPA.³⁰ The Tb EE slowly continues to increase with vortexing time, the Gd EE stays around 90 %. 10 minutes of vortexing was therefore optimal for extraction. As DEHPA is shown to be selective for Tb over Gd it was hypothesized that a shorter vortexing time might show better separation as the Tb would form a complex first. Because the concentrations of DEHPA and Gd greatly exceed the Tb concentration this is not observed here.

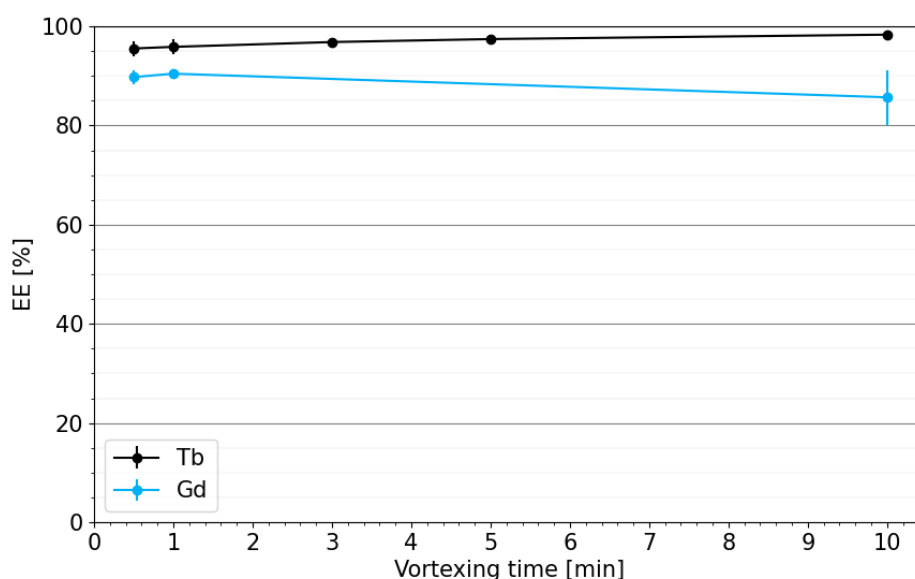


Figure 4.4: Extraction efficiencies [%] of Tb and Gd using 0.1 M DEHPA and aqueous phase at pH = 1.3. The extractions were carried out with 15 mM Gd and 0.15 mM Tb in HNO₃, PE 100-140 as the organic phase and various vortexing times. The error bars represent one standard deviation of the mean. The lines serve to guide the eyes but have no scientific meaning.

4.2.3. Organic phase

Three different organic solvents were investigated: PE 100-140, chloroform and benzene. In the extraction with benzene, the phases were difficult to separate after vortexing as their densities were very similar causing the formation of bubbles in the vial. This is undesired so benzene was quickly discarded as a solvent option. The Tb EEs of PE 100-140 and chloroform were 98.3 ± 0.5 % and 64.6 ± 0.4 % respectively. One possible explanation for the lower EE in chloroform is that it has a dielectric constant of 4.81 while petroleum ether has a dielectric constant of 2, both at 25°C.^{92,93} It has been reported that an increase in the dielectric constant of the diluent has a negative effect on the EE as the interaction between the diluent and the extractant is increased, thus decreasing the availability of the extractant for extraction.^{86,94} Another influencing factor is the solubility of the organic solvent in the aqueous phase. Chloroform is more soluble in water than PE 100-140, 0.815 wt % versus 0.004 wt % at 20°C.³³ They are both still highly insoluble so this cannot fully explain the difference in EE. Finally, their viscosity influences the vortexing phase of the extraction. A higher viscosity lowers the Reynolds number of the mixing system given in Equation 4.1 and subsequently lowers the tendency for turbulent mixing. Here Re is Reynolds number, the ratio between inertial and viscous forces, ρ is the density in kg/m³, u the flow speed in m/s, L a characteristic length and μ the dynamic viscosity in kg/(ms).

$$Re = \frac{\rho u L}{\mu} \quad (4.1)$$

A higher density increases the Reynolds number as opposed to a higher viscosity. PE 100-140 has a viscosity of 0.46 mPa s while chloroform has a higher viscosity of 0.542 mPa s at 25°C. The densities of PE 100-140 and chloroform are 0.74 and 1.49 g/mL respectively.⁹⁵ The Reynolds number of the chloroform extraction is therefore higher causing a more turbulent flow. Because the phase mixing is done on a vortexing machine for 10 minutes this influence is negligible and therefore the difference in EEs is attributed to the difference in dielectric constants. In microfluidic solvent extraction however, this does play a more important role. The choice of PE 100-140 as an organic phase also makes the extractions more reliable as chloroform is highly volatile and may evaporate partly during the extraction. It should be noted that PE 100-140 itself is not an ideal compound to use as it is toxic and flammable. Less dangerous solvents like ionic liquids as discussed in Section 2.3 may therefore be investigated in future research if required.

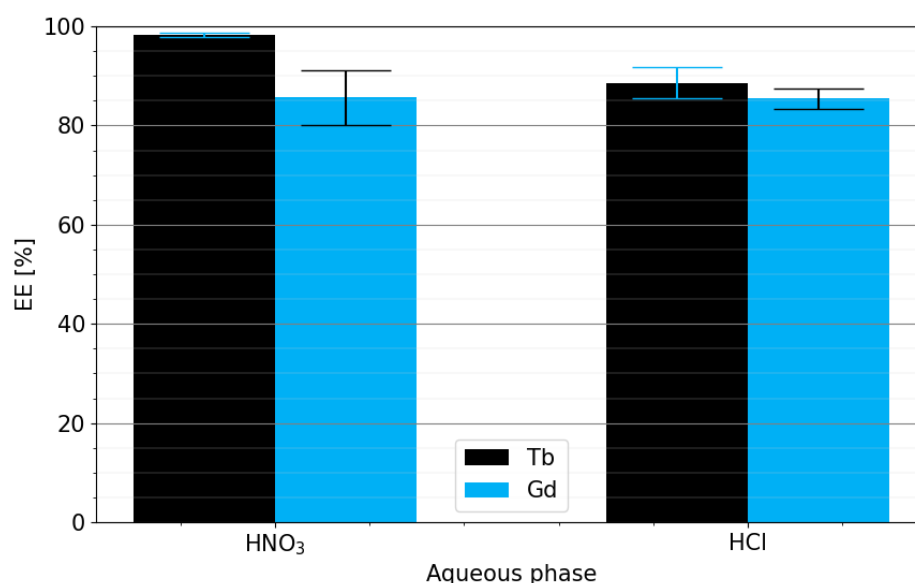


Figure 4.5: Extraction efficiency [%] of Tb and Gd using 0.1 M DEHPA in PE 100-140 with aqueous phase HNO₃ or HCl at pH = 1.3. The extractions were carried out with 15 mM Gd and 0.15 mM Tb and 10 minutes vortexing time. The error bars represent one standard deviation of the mean.

4.2.4. Aqueous phase

Both HNO_{3, aq} and HCl_{aq} were investigated as an aqueous phase. The extraction results are shown in Figure 4.5. It can be observed that the EEs for Gd for HCl and HNO₃ are not significantly different, 85.7 ± 5.5 % and 85.5 ± 2.1 % respectively. The Tb EE are significantly different however, 98.3 ± 0.5 % for HNO₃ and 88.6 ± 3.2 % for HCl. This can be explained by a speciation simulation done in CHEAQS. The used parameters are given in Table A.8 along with the relative amount of free and bounded Tb³⁺ and Gd³⁺. When using HNO₃ as an aqueous phase, there is less free Tb and so the complexation mechanism as discussed in Section 2.3.3 is important: one or two Cl⁻ or NO₃⁻ group(s) can replace a DEHPA dimer in the extraction meaning less DEHPA molecules are needed per Tb atom.⁶¹ This explains that more Tb can be extracted with less DEHPA when using HNO₃ as the aqueous phase. HNO₃ showed the best separation. Further investigation can be done by looking for other ions like NO₃⁻ that are selective for Tb over Gd or by increasing the NO₃⁻ concentration as this could increase their separation.

4.2.5. DEHPA concentration

Finally, the concentration of DEHPA was varied. Increasing it was expected to result in a higher Gd EE since the Tb EE is already high. The Gd concentration was therefore increased to 150 mM. The results of the extractions are shown in Figure 4.6. The EEs increase with DEHPA concentration as is expected and widely reported in literature.^{30,44,47,50,52,96,97} The difference in Tb and Gd EEs upon decreasing the DEHPA concentration stays about constant. It can also be observed that the ratio between the Gd and Tb concentration does not have much effect on their separation as long as the amount of DEHPA is sufficient; the EE of Tb goes from 98.6 ± 0.2 % to 93.1 ± 1.2 % and the EE of Gd from 85.7 ± 5.5 % to 77.1 ± 5.8 % when increasing the Gd amount. Increasing the DEHPA concentration should make up for the difference in EE for Tb. The fact that increasing the DEHPA concentration linearly with the Gd concentration does not give the same EE as before can be caused by a decrease in the amount of TbNO_{3, aq}²⁺. Another cause can be that DEHPA is much more viscous than PE 100-140 (56 mPa s versus 0.46 mPa s and increasing the amount of DEHPA and therefore the DEHPA/PE 100-140 ratio increases the viscosity of the organic phase by a significant amount.⁹⁸ This makes the mixing of the two phases more difficult and can have a negative effect on the EE.

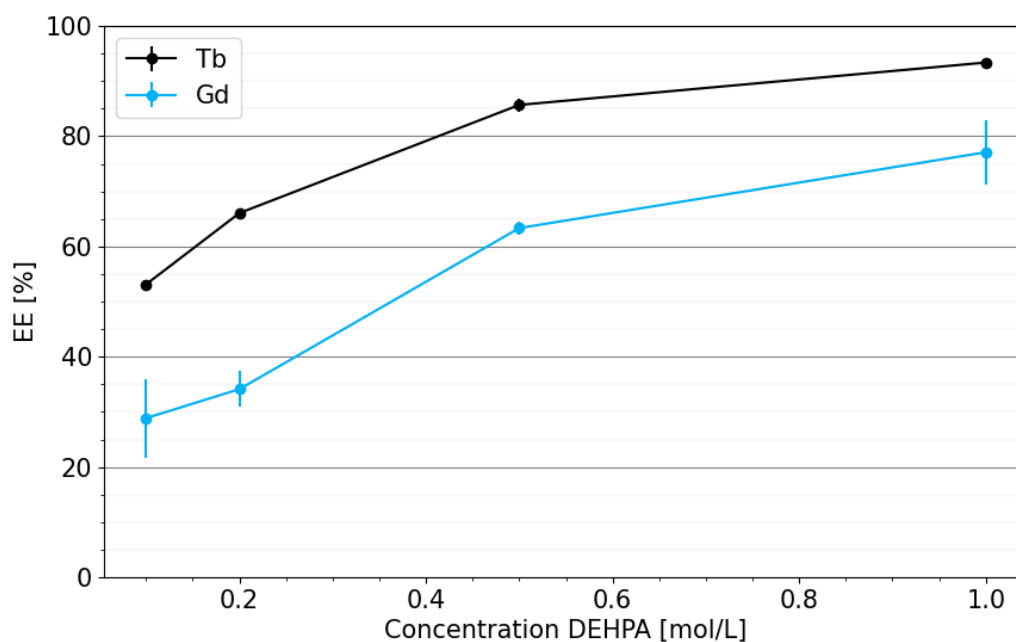


Figure 4.6: Extraction efficiencies [%] of Tb and Gd. The extractions were carried out with 150 mM Gd and 0.15 mM Tb in HNO_3 as the aqueous phase at $\text{pH} = 1.3$. Various concentrations of DEHPA in PE 100-140 were used as the organic phase and the vials were vortexed for 10 minutes. The error bars represent one standard deviation of the mean.

4.3. Back-extraction

As discussed in Section 2.3 in the back-extraction phase a strong acidic solution is added to the organic phase with extracted complex to break the complex and in turn back-extract the metal ions into the aqueous phase. The effective back-extraction or stripping of DEHPA-lanthanide complexes is known to be difficult and so a very acidic solution is required to back-extract most of the Tb and Gd.^{75,99,100} In Figure 4.7 the BEE of Tb is shown versus HNO_3 -based solutions in different concentrations as the back-extracting agent. Most Tb is back-extracted with 2 M HNO_3 or higher. A relatively low acidity of the back-extracting agent is desired as future applications require more dilute solutions. A highly acidic back-extracting agent would therefore have to be diluted considerably resulting in solutions with large volumes.

The BEE using HCl-based solutions was also investigated. HCl is a slightly stronger acid than HNO_3 and is therefore expected to have a higher BEE. Furthermore, after removing Gd using the solvent extraction system, the resulting solution has to be further purified using an ion exchange column which requires the lanthanides to be loaded in a 0.05 M HCl solution. The investigation of the BEE with HCl is therefore important. The results are shown in Figure 4.8. HCl indeed back-extracts more Tb than HNO_3 at both molarities. The BEEs are however very similar and so there is some freedom when selecting a back-extracting agent.

The BEE of Gd is assumed to be higher than that of Tb as less Gd is extracted at each pH. The DEHPA/Gd complex is less strong and is therefore expected to break more easily. An experiment with 2 M HNO_3 indeed yielded a near 100 % BEE for Gd. No additional separation is therefore possible in the back-extraction phase.

The investigation above yielded a Tb EE of 98.6 ± 0.2 % and a Gd EE of 85.7 ± 5.5 % followed by a Tb BEE of 98.2 ± 0.1 % and Gd BEE of more than 98.2 ± 0.1 % using the DEHPA extraction and subsequent 2 M HNO_3 back-extraction system. This is not sufficient as a standalone separation but the extraction system is now well understood. In the following section, the aqueous reverse-size selective

chelator MACROPA is investigated to increase the separation.

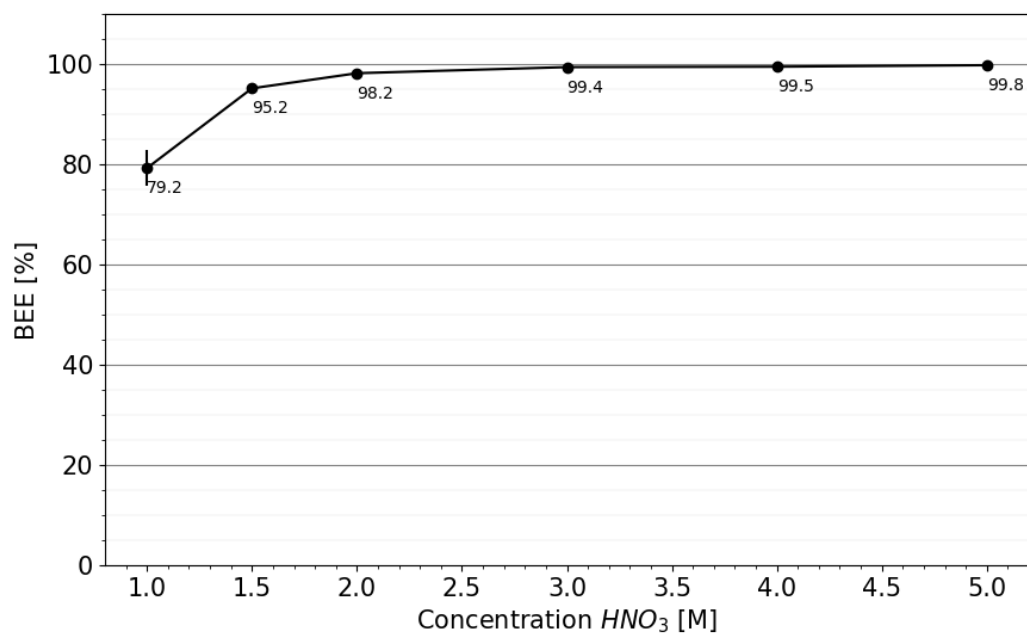


Figure 4.7: BEE % of Tb with various concentrations HNO₃ as the back-extracting agent. The vortexing time was 10 minutes and the error bars represent one standard deviation of the mean. The lines serve to guide the eyes but have no scientific meaning.

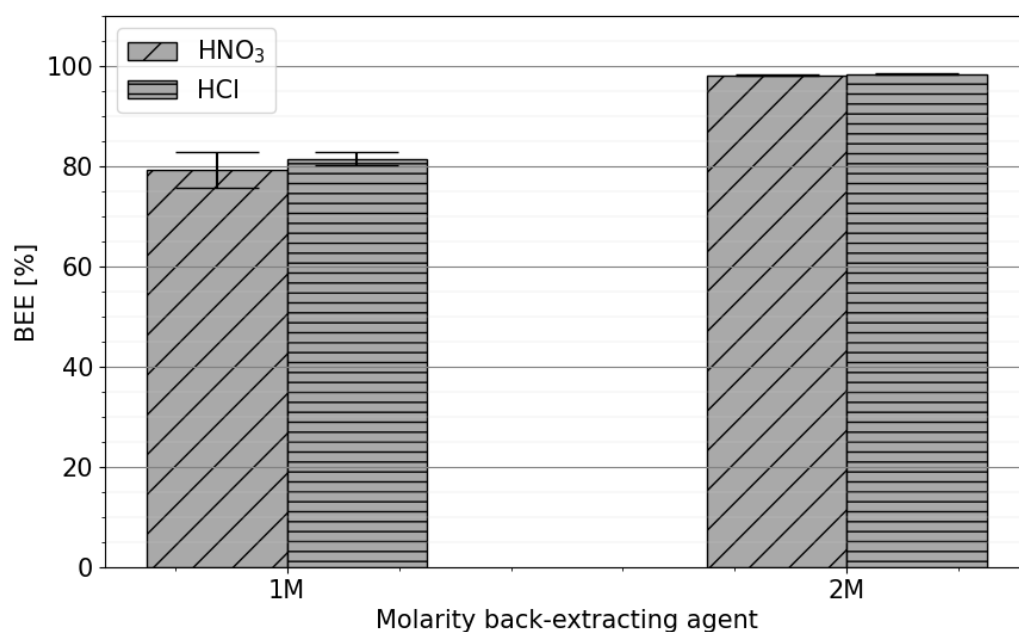


Figure 4.8: BEE [%] of Tb with various concentrations HNO₃ and HCl as the back-extracting agent. The vortexing time was 10 minutes and the error bars represent one standard deviation of the mean.

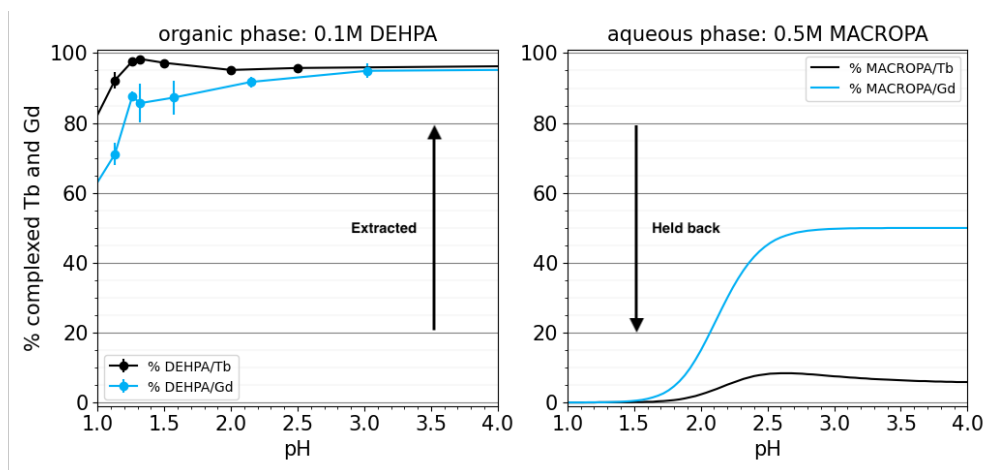


Figure 4.10: The simulated speciation results from Section 2.3.4 (right figure) next to the DEHPA extraction versus pH. The concentrations Tb and Gd are the same as in Figure 4.3, using 0.1 M DEHPA to extract and a simulated 0.5 M MACROPA to preferentially complex Gd in the aqueous phase. The lines in the left figure serve to guide the eyes but have no scientific meaning.

4.4. MACROPA/DEHPA extraction system

A system with extractant and hold-back agent has the potential to boost separation as discussed in Section 2.3.4 and as shown by Johnson et al. and Sun et al. who both used a similar so-called 'tug-of-war' strategy for the separation of lanthanides.^{19,63} Adding MACROPA to the DEHPA extraction system is not straightforward as a balance has to be found between the different complex strengths of MACROPA and DEHPA with Tb and Gd. In Figure 4.10 the DEHPA extraction versus pH is shown next to the simulated speciation results from Section 2.3.4. Here, the same concentrations Tb and Gd were used as in Figure 4.3 with the addition of 0.5 M MACROPA. Ideally, the MACROPA complex is stronger than that of DEHPA as it would then preferentially complex about 50% Gd and only 5-10% Tb. The remaining free Tb and Gd could then be extracted with the DEHPA. As the MACROPA needs a pH larger than 1.5 to form complexes the separative capabilities of DEHPA at lower pH cannot be utilized.

In Figure 4.9, the results of extractions using 0.005 M MACROPA and 0.001 M DEHPA and back-extraction with 2 M HNO₃ are shown for 100x diluted Tb/Gd aqueous solution at pH 2 and pH 3.5 for investigation of the pH dependence of the DEHPA/MACROPA system. It can be observed that the separation is greatly enhanced. At pH = 3.5, the EE of Tb is still high: 95.0 ± 0.2 % whilst the Gd has an EE of 53.1 ± 3.0 %. This means that the MACROPA/Gd complex is stronger than the DEHPA/Gd complex as nearly 50% is held back in the aqueous phase.

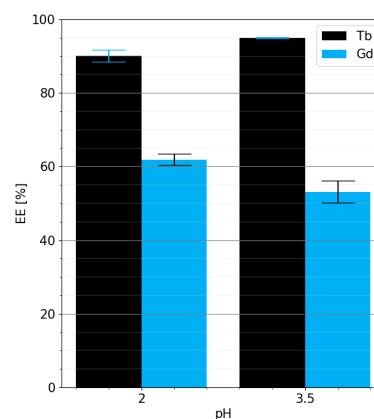


Figure 4.9: EEs of Tb and Gd using 0.005 M MACROPA and 0.001 M DEHPA and back-extraction with 2 M HNO₃ for 100x diluted Tb/Gd aqueous solution at pH 2 and pH 3.5, a vortexing time of 10 min and PE 100-140 as the organic phase. The error bars represent one standard deviation of the mean.

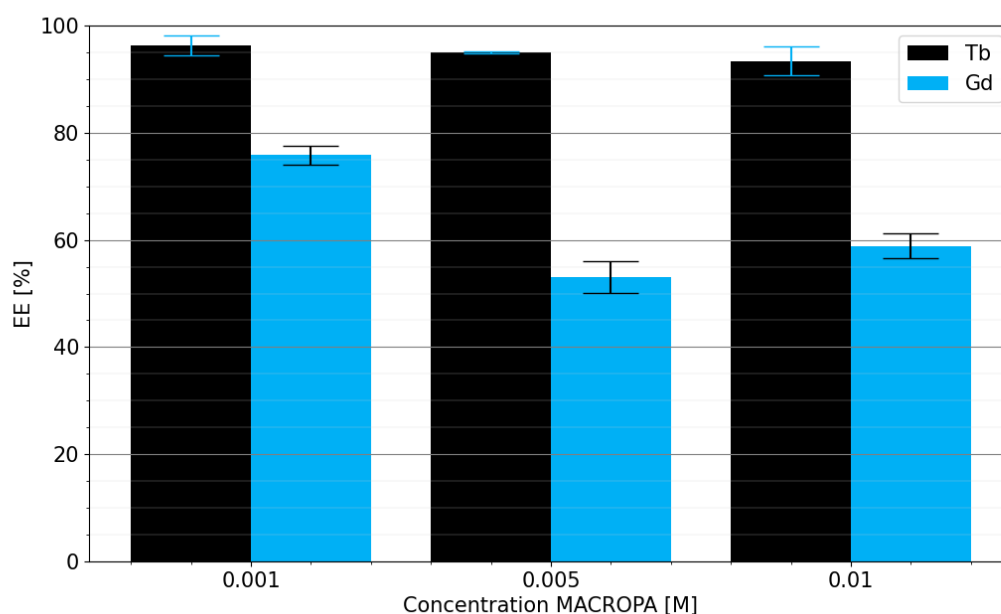


Figure 4.12: EEs of Tb and Gd using MACROPA and 0.001 M DEHPA and back-extraction with 2 M HNO_3 for 100x diluted Tb/Gd aqueous solution at pH 3.5, a vortexing time of 10 min and PE 100-140 as the organic phase versus various concentrations of MACROPA. The error bars represent one standard deviation of the mean.

In Figure 4.12, EEs using MACROPA and 0.001 M DEHPA and back-extraction with 2 M HNO_3 are shown for 100 times diluted Tb/Gd aqueous solution at pH = 3.5 with various concentrations of MACROPA in the aqueous phase. An increase in MACROPA concentration results in a decrease in Tb EE as more Tb is held back in the aqueous phase. The Gd EE also decreases with increasing MACROPA concentration but at very high concentrations it increases again which is unexpected. During experiments with higher concentrations of Tb, Gd, DEHPA, and MACROPA a third phase formed after vortexing as shown in Figure 4.11. At lower MACROPA concentrations, both before vortexing and some time after vortexing, this was not the case and so it is attributed to the lower solubility of the MACROPA/Tb and MACROPA/Gd complexes in an aqueous phase with high ionic strength. As it did not occur at lower MACROPA concentrations the data shown in this section is not affected in any way by this third phase formation. If higher amounts of MACROPA are required it is recommended to use larger aqueous phase volumes to avoid this problem.

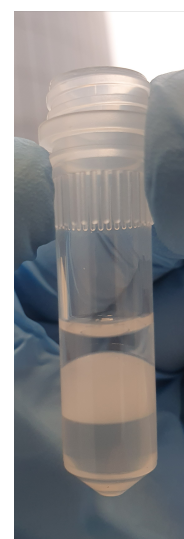


Figure 4.11: The formation of a third phase after vortexing in experiments with higher concentrations MACROPA.

Since the concentrations Tb and Gd can only be measured before adding the MACROPA and after back-extraction due to restrictions of the ICP-MS detector the specific behaviour of the system during extraction is hard to investigate. Other quantitative measurement techniques like instant thin layer chromatography (iTLC) or high-pressure liquid chromatography (HPLC) in combination with UV-Vis to obtain information about the complexation of MACROPA with Tb and Gd therefore have to be looked at in future research to be able to fully understand and optimize the system.

The relations between EEs and pH and MACROPA concentration were also observed by Thiele et al. where a similar system but with different aqueous phase, organic phase and MACROPA concentrations were used in the separation of lighter lanthanides (La - Eu).²⁰ In this thesis, we have shown

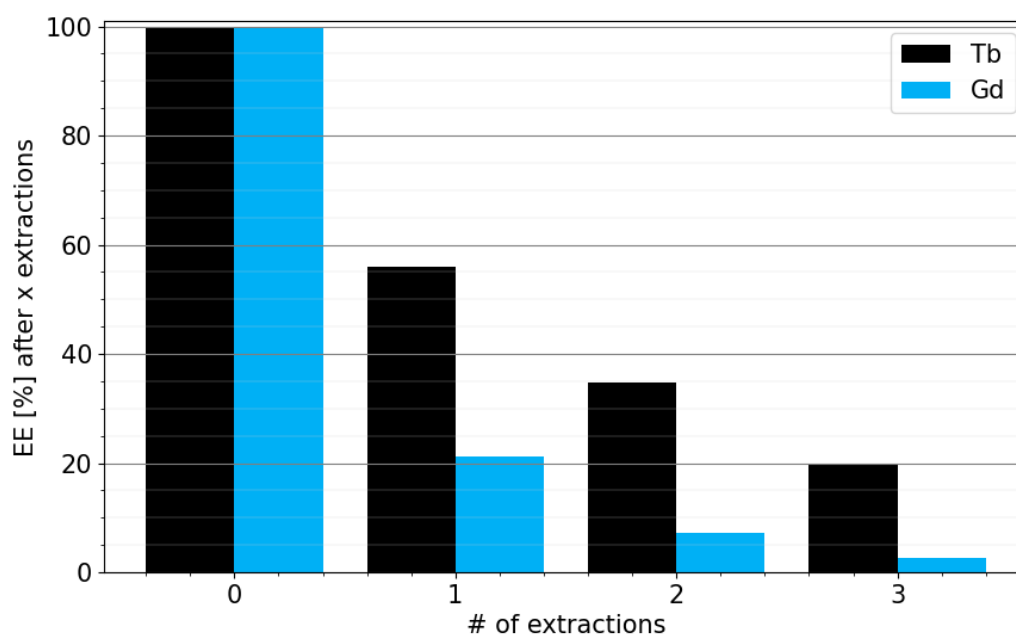


Figure 4.13: The results of repeating the MACROPA/DEHPA extraction system: 0.005 M MACROPA and 0.001 M DEHPA, back-extraction with 2 M HNO₃ for 100x diluted Tb/Gd aqueous solution at pH 3.5 as a starting solution, a vortexing time of 10 min and PE 100-140 as the organic phase. Values shown are total EEs after each step.

that this use of MACROPA as a hold-back agent can be extended to the most difficult to separate lanthanides, Tb and Gd, using the DEHPA extraction system developed in Section 4.2. Moreover, the separation factor of 16.8 ± 1.6 for Tb and Gd is amongst the highest ever reported.

Finally, it was investigated whether the developed extraction system can be performed multiple times in sequence to increase the separation even more. As most Tb is extracted, this should not lead to much loss of Tb but should decrease the amount of Gd that is in the solution. To do this however, the pH of the solution after back-extraction must be raised to where the extraction is optimal. This can be tricky as the back-extracting agent is very acidic so volumes of 5 mL were used as aqueous and organic phases to facilitate this. The results of doing this twice (so three extractions in total) are shown in Figure 4.13. A few things can be observed. First, the EE of the experiments were very similar so the extraction pH and therefore the extraction conditions of the various experiments were similar enough for similar extraction results, see Figure 4.14. Second, the overall EEs, especially for Tb are lower than desired. This can either be caused by an excess of MACROPA or a lack of DEHPA or by the vortexing manner and has to be fixed to lower losses of Tb in the extraction procedure. The vortexing differed from before as the volumes were larger but the same vortexing time was used. There is a possibility that this time was not sufficient, leading to a lower EE. The relative amount of MACROPA was higher in every extraction including the first as the same concentration was used for every extraction. This meant that more Gd and Tb could have formed a complex with MACROPA and could therefore not be extracted resulting in a lower EE. All in all however, this experiment does demonstrate the possibility of using subsequent extractions to separate a bulk of Gd from Tb in a couple of extractions. The EE of Tb was approximately 10 times as large as the Gd EE after the third extraction (20 % Tb versus 2 % Gd). To see whether the final product can still be used in ion exchange column chromatography for further separation two experiments will be done: one with the diluted product of the MACROPA/DEHPA extraction and subsequent back-extraction and one with a clean loading solution for comparison. The results of these experiments are discussed in the next section (4.5).

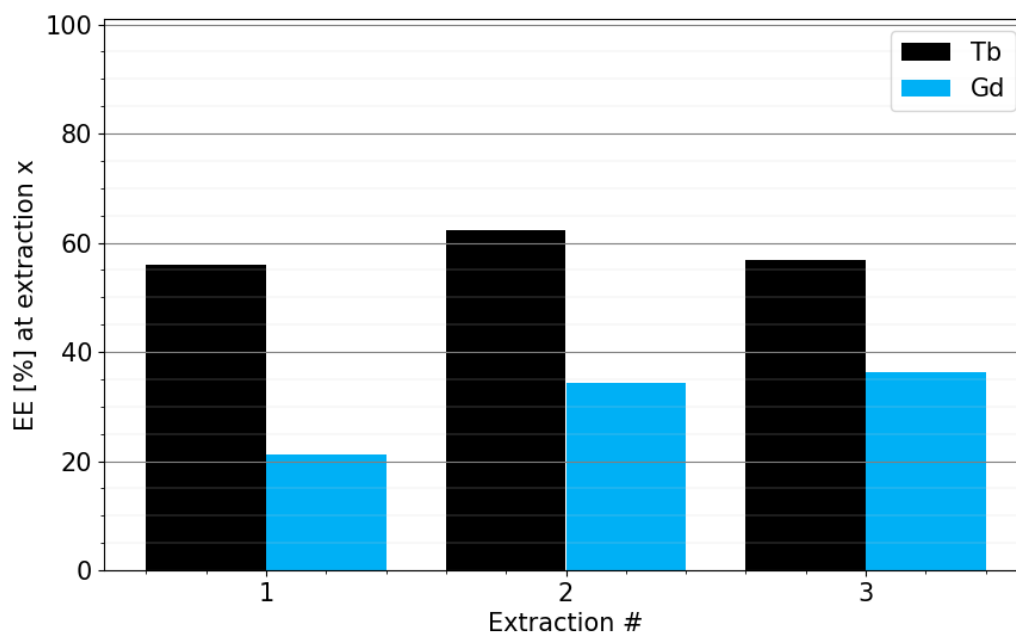


Figure 4.14: The results of repeating the MACROPA/DEHPA extraction system: 0.005 M MACROPA and 0.001 M DEHPA, back-extraction with 2 M HNO_3 for 100x diluted Tb/Gd aqueous solution at pH 3.5 as a starting solution, a vortexing time of 10 min and PE 100-140 as the organic phase. Values shown are EEs for each extraction.

4.5. Ion exchange column chromatography

As mentioned before, ion exchange column chromatography can be used to further separate Gd and Tb. The used method and columns were developed by Triskem.^{17,69} Two experiments were carried out to investigate whether the final product of the DEHPA/MACROPA extraction system can be used as a loading solution for the TK212 column: one with the diluted product of the MACROPA/DEHPA extraction and subsequent back-extraction and one with a clean loading solution for comparison. These solutions were prepared as discussed in Section 3.2.4. The result of the separation with the clean loading solution is shown in Figure 4.15. The separation is very good, there is no overlap of the peaks and most of the eluted masses are in their respective peaks: 99.4 % Gd in fractions 4-18, 99.2 % Tb in fractions 35-42, and 98.6 % Dy in fractions 43-55. This result is in good accordance with results obtained by Triskem.^{17,69} In Figure 4.16, the result of the separation using the diluted experiment end product loading solution is shown. The separation is also very good, there is no overlap of the peaks and most of the eluted masses are in their respective peaks: 99.6 % Gd in fractions 9-29 and nearly 100 % Tb in fractions 34-44. This result shows that the column separation still works after doing a prior extraction to remove the Gd bulk. There is one difference between the two measurements: the Gd is eluted later than before. Most of it was breaking through during the load with the clean loading solution. In the other experiment, it only showed from fraction 12 onwards, after starting to elute with 0.2 M HNO_3 . This can be explained by the lower amount of Gd that is being loaded and eluted. As some Gd is expected to interact with the resin inside the column it would only be flushed out after elution.

To check that there was indeed no difference between the clean loading solution and the diluted experiment loading solution their UV-Vis spectra were measured along with a clean solution containing MACROPA and a DEHPA in PE 100-140 solution. Any variation between the spectra of the two solutions could be attributed to the presence of MACROPA or DEHPA. This is shown in Figure 4.17. The experiment solution overlaps the clean solution and the DEHPA in PE 100-140 solution. The MACROPA shows a different absorbance in the lower wavelength region. We therefore conclude that no measurable amount of MACROPA is present in the experiment solution. We cannot conclude the same for DEHPA since the spectra overlap but as the column separation shows no difference we also expect

the amount of DEHPA in the experiment solution to be low.

Finally, it must be noted that the amount of waste, both plastic and fluids is very large in the column separation procedure compared to the solvent extraction separation. The time periods in which the separations can be done also differ considerably: approximately 1 hour for solvent extraction versus approximately 8 hours for column separation including regeneration. This shows once more why the development of a fast removal procedure of the Gd bulk is important.

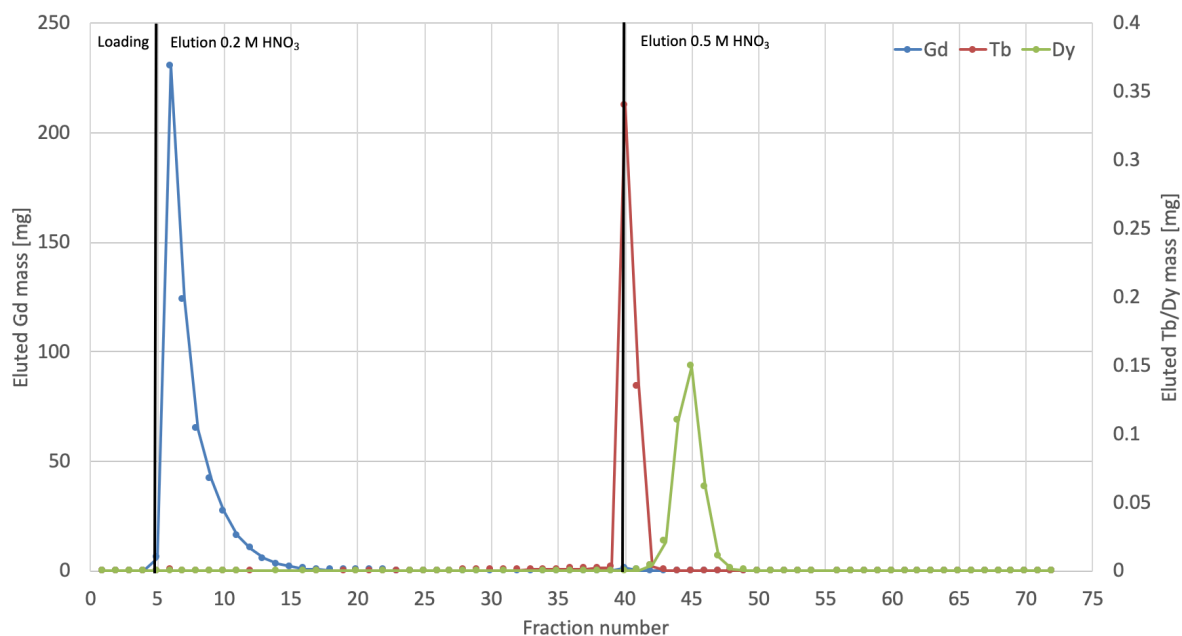


Figure 4.15: The elution of a clean loading solution (0.05 M HCl) containing 500 mg Gd, 500 μg Tb and 500 μg Dy on the TK212 column. The fraction volume is 40 mL.

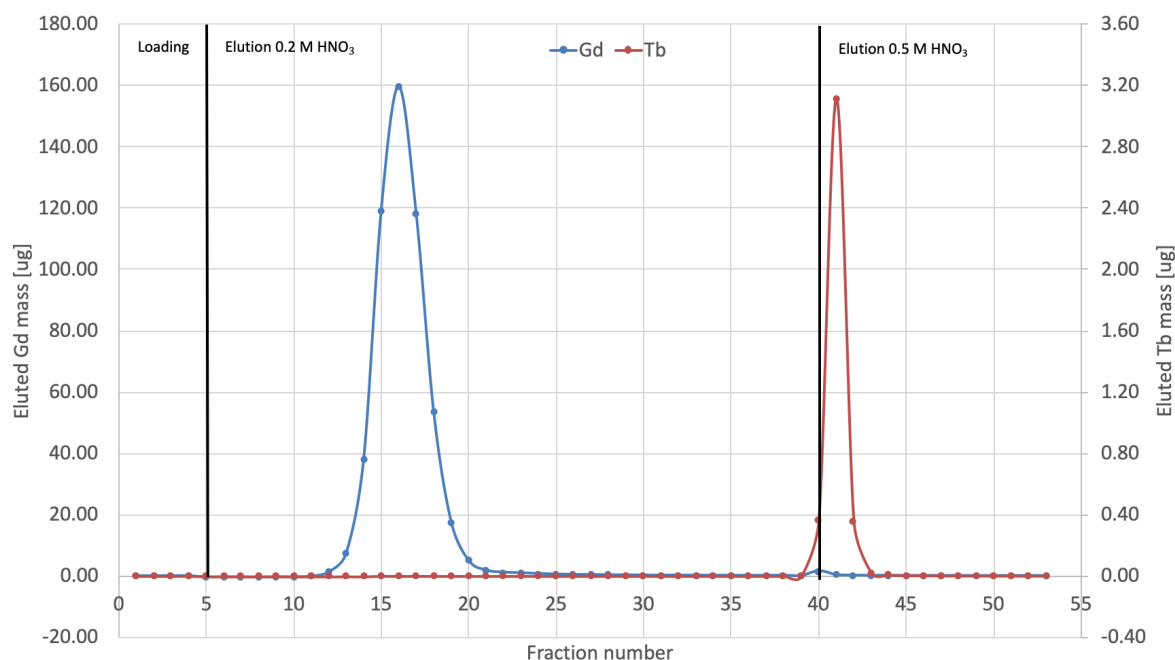


Figure 4.16: The elution of the diluted experiment end product loading solution (0.05 M HCl) containing 500 μg Gd and 4 μg Tb on the TK212 column. The fraction volume is 40 mL.

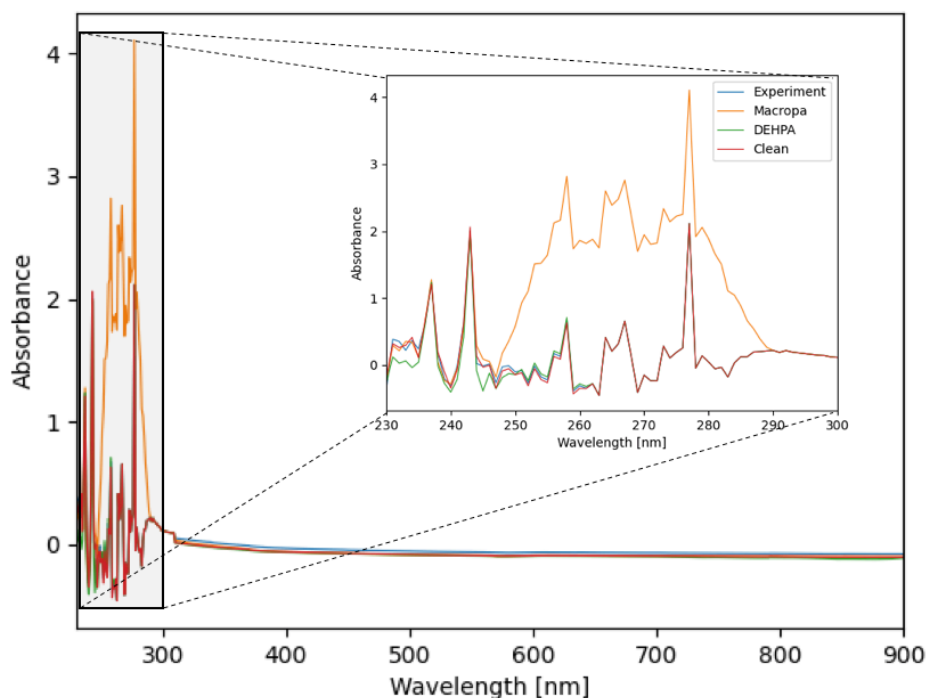


Figure 4.17: The UV-Vis spectrum of various compounds, only the MACROPA spectrum differs from the other measured solutions.

4.6. Gadolinium and MACROPA recycling

As discussed in the introduction, the enriched Gd required for irradiation is expensive and is ideally recycled so that it can be irradiated again. The same goes for the MACROPA, it is also ideally reused since it is hard to come by. In this section, the possibilities for doing this are discussed.

For Gd, the first and easiest option would be to precipitate it with something as that would allow for quick separation from the aqueous phase. The precipitation of Gd has been shown to be easily possible with, amongst others, phosphates or oxalates, even at lower pH.^{101–104} Since the pH of the remaining aqueous solution after extraction contains MACROPA complexes of Gd this complex must be destroyed first by lowering the pH, re-raising it to a value around 1 to avoid the formation of MACROPA complexes and adding phosphoric acid could then allow for precipitation of Gd. The precipitation at lower pH is lower than at higher pH and it must therefore be investigated whether this will work.¹⁰²

A second option is to lower the pH to break the MACROPA/Gd complex as before and then do an extraction with the DEHPA system at low pH (± 1.5). Most Gd and Tb should then be extracted by the DEHPA and what would remain is an aqueous phase containing only MACROPA. This could then either be dried down to recover the MACROPA or reused as an aqueous phase for another extraction. It is advised to investigate this in future research.

5

Conclusion

^{161}Tb is considered a promising alternative to ^{177}Lu in the treatment of neuroendocrine tumors and prostate cancer.¹⁻⁶ It has only recently become commercially available with high levels of purity, but up-scaling its production is still an ongoing area of research since its demand is expected to keep growing.¹¹ It is produced via neutron irradiation of ^{160}Gd targets and its subsequent separation from said targets. Current separation methods cannot handle large amounts of irradiated Gd at a time, separation times are quite lengthy (mL/min) and the required columns are large. A fast removal method of the Gd bulk is therefore desired and was developed in this research. The main conclusions from this research will now be summarized and recommendations for future research will also be discussed.

Three possible extractants, DEHPA, PC-88A, and a combination of DDPA and TBP were investigated for the extraction and separation of Tb and Gd. DEHPA and PC-88A extracted high amounts of Tb (EEs of $98.3 \pm 0.5\%$ and $98.6 \pm 0.2\%$ respectively) whilst DDPA with TBP did not ($EE = 73.6 \pm 2.5\%$). DEHPA extracted lower amounts of Gd than PC-88A at all measured conditions and was therefore selected as the to-be-optimized extractant. The DEHPA extraction system was further optimized by varying the pH of the aqueous phase, the vortexing time, the type of organic phase, the type of aqueous phase and the DEHPA concentration.

A lower pH of the aqueous phase was found to have a negative effect on the EEs of both Tb and Gd mainly caused by the protonation of DEHPA at lower pH. The EEs unexpectedly dropped slightly at pH 1.5 and higher which could be caused by the presence of Na^+ ions in the solution or by a temperature difference between lower and higher pH experiments. The presence of Na^+ ions reduces the amount of $\text{GdNO}_{3\text{aq}}^{2+}$ and $\text{TbNO}_{3\text{aq}}^{2+}$ and in turn lowers the EE as discussed in Sections 2.3.3 and 4.2.4. The temperature dependency has to be further investigated. The optimal pH for Tb/Gd separation was found to be 1.3.

A longer vortexing time was found to increase EE, 10 minutes was deemed optimal, but high EEs were already reported at 30 seconds.

PE 100-140 was found to be the best-tested organic phase for the extraction. The density of benzene was too similar to the aqueous phase making phase separation difficult. The Tb EE of chloroform was lower than that of PE 100-140 caused by its higher dielectric constant and subsequent increased interaction with the extractant. Since PE 100-140 is a toxic and flammable solvent, it is advised to investigate less dangerous solvents like ionic liquids in future research if required.

$\text{HNO}_{3,\text{aq}}$ was found to be a better aqueous phase for the extraction than HCl_{aq} since HCl_{aq} had a lower Tb EE than $\text{HNO}_{3,\text{aq}}$ ($98.3 \pm 0.5\%$ versus $88.6 \pm 3.2\%$). This could be caused by the increase in free Tb in HCl_{aq} compared to $\text{HNO}_{3,\text{aq}}$ thereby limiting the complexation and extraction mechanism discussed in Section 2.3.3 and requiring more DEHPA for the same EE.

An increase in DEHPA concentration was found to have a positive effect on the EEs of both Tb and Gd.

Finally, it was found that most, > 98 % Tb (and Gd), is back-extracted using 2 M HNO₃ or HCl-based solutions and 10 minutes vortexing time.

The DEHPA extraction system yielded a Tb EE of 98.6 ± 0.2 % and a Gd EE of 85.7 ± 5.5 % followed by a Tb BEE of 98.2 ± 0.1 % and Gd BEE of more than 98.2 ± 0.1 %. This was boosted by adding the reverse size selective chelator MACROPA to the aqueous phase to hold back the Gd. Optimization of this combined DEHPA/MACROPA extraction system for pH and MACROPA concentration yielded a Tb EE of 95.0 ± 0.2 % and a Gd EE of 53.1 ± 3.0 % thereby showing that the use of MACROPA as a hold-back agent as reported by Thiele et al.²⁰ can be extended to the separation of the most difficult to separate lanthanides. Moreover, the separation factor of 16.8 ± 1.6 for Tb and Gd is amongst the highest ever reported. The extraction was performed multiple times in sequence to further increase the separation. The ratio between total EEs of Tb and Gd after three subsequent extractions was approximately 10 demonstrating the potential of using sequential extractions to remove a bulk of Gd from Tb. The procedure of doing consecutive extractions must however be further optimized as nearly 80% of Tb was not extracted. Finally, the solution after extraction and back-extraction using the DEHPA/MACROPA system was loaded onto the TK212 column developed by Triskem to verify if purification using the column was still possible. There were no considerable differences between a clean loading solution and the loading solution after the initial separation showing that the column separation procedure still works after doing a prior extraction to remove the Gd bulk.

As discussed in Section 4.6, it is highly advised to investigate the recycling of Gd and MACROPA from the aqueous phase after extraction. As the TK212 column separates based on a resin that consists of different mixtures of organophosphoric, organophosphonic, and organophosphinic acids it could be investigated whether this mixture has more separation capabilities than DEHPA as an extractant. Finally, the automation of the extraction system can be investigated in an attempt to further speed up ¹⁶¹Tb production.

References

- ¹S. Lehenberger, C. Barkhausen, S. Cohrs, E. Fischer, J. Grünberg, A. Hohn, U. Köster, R. Schibli, A. Türlér, and K. Zhernosekov, “The low-energy beta- and electron emitter ^{161}Tb as an alternative to ^{177}Lu for targeted radionuclide therapy”, *Nuclear Medicine and Biology* **38**, 917–924 (2011).
- ²N. Gracheva, C. Müller, Z. Talip, S. Heinitz, U. Koester, J. Zeevaart, A. Vögele, R. Schibli, and N. van der Meulen, “Production and characterization of no-carrier-added ^{161}Tb as an alternative to the clinically-applied ^{177}Lu for radionuclide therapy”, *EJNMMI Radiopharmacy and Chemistry* **4**, 10.1186/s41181-019-0063-6 (2019).
- ³H. Golan, *Radiopharmacy and radiobiology aspects for 161-terbium*, Oct. 2023.
- ⁴C. Müller, N. P. van der Meulen, and R. Schibli, “Opportunities and potential challenges of using terbium-161 for targeted radionuclide therapy in clinics”, *European Journal of Nuclear Medicine and Molecular Imaging* **50**, 3181–3184 (2023).
- ⁵I. Cassells, S. Ahenkorah, A. R. Burgoyne, M. Van de Voorde, C. M. Deroose, T. Cardinaels, G. Bormans, M. Ooms, and F. Cleeren, “Radiolabeling of human serum albumin with terbium-161 using mild conditions and evaluation of in vivo stability”, *Frontiers in Medicine* **8**, 10.3389/fmed.2021.675122 (2021).
- ⁶A. Schaefer-Schuler, C. Burgard, A. Blickle, S. Maus, C. Petrescu, S. Petto, M. Bartholomä, T. Stemler, S. Ezziddin, and F. Rosar, “[^{161}Tb]tb-psma-617 radioligand therapy in patients with mcrcp: preliminary dosimetry results and intra-individual head-to-head comparison to [^{177}Lu]lu-psma-617”, *Theranostics* **14**, doi:10.7150/thno.92273 (2024).
- ⁷D. Mankoff, “Why nuclear imaging and radiotherapy?”, in *Radiopharmaceutical chemistry* (Springer International Publishing, Cham, 2019), pp. 3–10.
- ⁸W. N. Association, *Radioisotopes in medicine*, 2023.
- ⁹C. Courier, *Terbium: a new “swiss army knife” for nuclear medicine*, May 2022.
- ¹⁰C. Müller, K. Zhernosekov, U. Köster, K. Johnston, H. Dorrer, A. Hohn, N. T. van der Walt, A. Türlér, and R. Schibli, “A unique matched quadruplet of terbium radioisotopes for pet and spect and for alpha and beta-radionuclide therapy: an in vivo proof-of-concept study with a new receptor-targeted folate derivative”, *Journal of Nuclear Medicine* **53**, 1951–1959 (2012).
- ¹¹TerThera.
- ¹²F. Tárkányi, A. Hermanne, S. Takács, F. Ditroi, J. Csikai, and A. Ignatyuk, “Cross-section measurement of some deuteron induced reactions on ^{160}Gd for possible production of the therapeutic radionuclide ^{161}Tb ”, *Journal of Radioanalytical and Nuclear Chemistry* **298**, 10.1007/s10967-013-2507-x (2013).
- ¹³A. Chicheportiche, S. Ben-Haim, S. Grozinsky-Glasberg, K. Oleinikov, A. Meirovitz, D. J. Gross, and J. Godefroy, “Dosimetry after peptide receptor radionuclide therapy: impact of reduced number of post-treatment studies on absorbed dose calculation and on patient management”, *EJNMMI Physics* **7**, 5 (2020).
- ¹⁴M. Veiga, P. Mattiazzi, J. S. de Gois, P. C. Nascimento, D. L. Borges, and D. Bohrer, “Presence of other rare earth metals in gadolinium-based contrast agents”, *Talanta* **216**, 120940 (2020).
- ¹⁵J. A. Peters, K. Djanashvili, C. F. Geraldes, and C. Platas-Iglesias, “The chemical consequences of the gradual decrease of the ionic radius along the Ln-series”, *Coordination Chemistry Reviews* **406**, 213146 (2020).
- ¹⁶J. M. Regenstein and C. E. Regenstein, “Chapter 15 - column chromatography”, in *Food protein chemistry*, edited by J. M. Regenstein and C. E. Regenstein (Academic Press, 1984), pp. 144–167.
- ¹⁷S. Happel, “Triskem infos”, edited by M. Langer (2020).

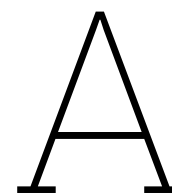
- ¹⁸A. Aziz, "Physico-chemical characterization of the terbium-161 radioisotope through separation based on cartridge In resin column from irradiated of enriched gd2o3 target", *Journal of Physics: Conference Series* **1436**, 012097 (2020).
- ¹⁹K. R. Johnson, D. M. Driscoll, J. T. Damron, A. S. Ivanov, and S. Jansone-Popova, "Size selective ligand tug of war strategy to separate rare earth elements", *JACS Au* **3**, 584–591 (2023).
- ²⁰N. A. Thiele, D. J. Fiszbein, J. J. Woods, and J. J. Wilson, "Tuning the separation of light lanthanides using a reverse-size selective aqueous complexant", *Inorganic Chemistry* **59**, 16522–16530 (2020).
- ²¹A. I. Kassis and S. J. Adelstein, "Radiobiologic principles in radionuclide therapy", *Journal of Nuclear Medicine* **46**, 4S–12S (2005).
- ²²J. van den Eijnde and L. Roobol, *Practical radiation protection* (Syntax Media, 2018).
- ²³NIBIB, *Nuclear medicine*, July 2016.
- ²⁴A. Khan and R. T. M. de Rosales (Torres Martin de Rosales), "Radiolabelling of extracellular vesicles for pet and spect imaging", *Nanotheranostics* **5**, 256–274 (2021).
- ²⁵G. Choppin, J. Liljenzin, J. Rydberg, and C. Ekberg, *Radiochemistry and nuclear chemistry* (Elsevier Science, 2013).
- ²⁶V. M. Denisov and I. A. Galkin, "Approximate cost of gadolinium-157 isotope production on cascade of liquid centrifuges", in 5 all-russian (international) scientific conference physicochemical processes during selection of atoms and molecules collection of reports (2000), p. 212.
- ²⁷R. de Kruijff, *Chemical methods for radionuclide separation*, Oct. 2023.
- ²⁸A. D. McNaught and A. Wilkinson, *Compendium of chemical terminology: iupac recommendations* (Blackwell Science, 1997).
- ²⁹D. C. Harris and C. A. Lucy, *Quantitative chemical analysis* (Freeman Custom Publishing, 2016).
- ³⁰A. Kumari, R. Panda, J. Y. Lee, T. Thriveni, M. K. Jha, and D. D. Pathak, "Extraction of rare earth metals (rems) from chloride medium by organo-metallic complexation using d2ehpa", *Separation and Purification Technology* **227**, 115680 (2019).
- ³¹D. W. Green and R. H. Perry, *Liquid-liquid extraction and other liquid-liquid operations and equipment*, 8th ed. (McGraw Hill Professional, 2007).
- ³²T. Goto and M. Smutz, "Separation factors for solvent extraction processes", *Journal of Inorganic and Nuclear Chemistry* **27**, 1369–1379 (1965).
- ³³V. S. Kislik, *Solvent extraction classical and novel approaches* (Elsevier, 2012).
- ³⁴L. Maria, A. Cruz, J. M. Carretas, B. Monteiro, C. Galinha, S. S. Gomes, M. F. Araújo, I. Paiva, J. Marçalo, and J. P. Leal, "Improving the selective extraction of lanthanides by using functionalised ionic liquids", *Separation and Purification Technology* **237**, 116354 (2020).
- ³⁵O. I. A. A. N. Turanov V. K. Karandashev and E. Sharova, "Solvent extraction of lanthanides(iii) from nitric acid solutions with novel functionalized ionic liquids based on the carbamoyl(methyl)phosphine oxide pattern in molecular diluents", *Solvent Extraction and Ion Exchange* **40**, 203–215 (2022).
- ³⁶A. Turanov, V. Karandashev, and M. Boltoeva, "Solvent extraction of intra-lanthanides using a mixture of tbp and todga in ionic liquid", *Hydrometallurgy* **195**, 105367 (2020).
- ³⁷F. Kubota and M. Goto, "Application of ionic liquids to solvent extraction", *Solvent Extraction Research and Development* **13**, 23–36 (2006).
- ³⁸K. NAKASHIMA, F. KUBOTA, T. MARUYAMA, and M. GOTO, "Ionic liquids as a novel solvent for lanthanide extraction", *Analytical Sciences* **19**, 1097–1098 (2003).
- ³⁹P. K. Parhi, "Supported liquid membrane principle and its practices: a short review", *Journal of Chemistry* **2013**, 1–11 (2013).
- ⁴⁰J. Doležal, C. Moreno, A. Hrdlička, and M. Valiente, "Selective transport of lanthanides through supported liquid membranes containing non-selective extractant, di-(2-ethylhexyl)phosphoric acid, as a carrier", *Journal of Membrane Science* **168**, 175–181 (2000).

- ⁴¹H. Matsuyama, K. Komori, and M. Teramoto, "Selectivity enhancement in the permeation of rare earth metals through supported liquid membranes by addition of diethylenetriaminepentaacetic acid to the aqueous phase", *Journal of Membrane Science* **47**, 217–228 (1989).
- ⁴²A. Hu and J. J. Wilson, "Advancing chelation strategies for large metal ions for nuclear medicine applications", *Accounts of Chemical Research* **55**, PMID: 35230803, 904–915 (2022).
- ⁴³M. Špadina, K. Bohinc, T. Zemb, and J.-F. Dufèvre, "Synergistic solvent extraction is driven by entropy", *ACS Nano* **13**, PMID: 31710459, 13745–13758 (2019).
- ⁴⁴T. Sato, "Liquid-liquid extraction of rare-earth elements from aqueous acid solutions by acid organophosphorus compounds", *Hydrometallurgy* **22**, 121–140 (1989).
- ⁴⁵T. SATO, S. BAN, and K. SATO, "Liquid-liquid extraction of rare-earth elements from hydrochloric acid solutions by di-(2-ethylhexyl)-phosphoric acid in the presence of pyridine or its derivatives.", *Shigen-to-Sozai* **115**, 252–256 (1999).
- ⁴⁶V. Innocenzi, N. M. Ippolito, L. Pietrelli, M. Centofanti, L. Piga, and F. Vegliò, "Application of solvent extraction operation to recover rare earths from fluorescent lamps", *Journal of Cleaner Production* **172**, 2840–2852 (2018).
- ⁴⁷L. Pechen and O. Sinigribova, "Extraction of gd, tb, and dy from nitrate media with a mixture of technical di-2-ethylhexyl phosphoric acid and tributylphosphate", *Theoretical Foundations of Chemical Engineering* **51**, 850–857 (2017).
- ⁴⁸A. Kandil and K. Farah, "The solvent extraction of terbium and europium by di-(2-ethylhexyl)-phosphoric acid and various organophosphorous compounds", *Journal of Inorganic and Nuclear Chemistry* **42**, 277–280 (1980).
- ⁴⁹J. Kurihara, "Liquid-liquid equilibria of terbium and dysprosium with pc-88a as extractant", PhD thesis (2012).
- ⁵⁰S. Radhika, B. N. Kumar, M. L. Kantam, and B. R. Reddy, "Liquid-liquid extraction and separation possibilities of heavy and light rare-earths from phosphoric acid solutions with acidic organophosphorus reagents", *Separation and Purification Technology* **75**, 295–302 (2010).
- ⁵¹V. Chiola, T. K. Kim, R. E. Long Jr, and B. C. Martin, "Solvent extraction process for separating gadolinium from terbium and dysprosium.", (1971).
- ⁵²F. Xie, T. A. Zhang, D. Dreisinger, and F. Doyle, "A critical review on solvent extraction of rare earths from aqueous solutions", *Minerals Engineering* **56**, 10–28 (2014).
- ⁵³Y. Wang, F. Li, Z. Zhao, Y. Dong, and X. Sun, "The novel extraction process based on cyanex® 572 for separating heavy rare earths from ion-adsorbed deposit", *Separation and Purification Technology* **151**, 303–308 (2015).
- ⁵⁴M. A. Afonin, A. V. Nechaev, I. A. Yakimenko, and V. V. Belova, "Extraction of rare earth elements from chloride solutions using mixtures of p507 and cyanex 272", *Compounds* **4**, 172–181 (2024).
- ⁵⁵S. Pavon, M. Kutucu, M. T. Coll, A. Fortuny, and A. M. Sastre, "Comparison of cyanex 272 and cyanex 572 for the separation of neodymium from a nd/tb/dy mixture by pertraction", *Journal of Chemical Technology & Biotechnology* **93**, 2152–2159 (2018).
- ⁵⁶S. Dashti, F. Rashchi, S. Shakibania, F. Sadri, and A. Ghahreman, "Separation and solvent extraction of rare earth elements (pr, nd, sm, eu, tb, and er) using tbp and cyanex 572 from a chloride medium", *Minerals Engineering* **161**, 10.1016/j.mineng.2020.106694 (2020).
- ⁵⁷S. Rizk, R. Gamal, and N. El-Hefny, "Insights into non-aqueous solvent extraction of gadolinium and neodymium from ethylene glycol solution using cyanex 572", *Separation and Purification Technology* **275**, 119160 (2021).
- ⁵⁸A. Saputra, K. T. Basuki, A. Rohmaniyah, and W. R. Pusparini, "Extraction development for the separation of gadolinium from yttrium and dysprosium concentrate in nitric acid using cyanex 572", *International Journal of Technology* **11**, 450–460 (2020).
- ⁵⁹N. Devi, K. Nathsarma, and V. Chakravorty, "Sodium salts of d2ehpa, pc-88a and cyanex-272 and their mixtures as extractants for cobalt(ii)", *Hydrometallurgy* **34**, 331–342 (1994).

- ⁶⁰D. J. Pruet, "Symposium of separation science and technology for energy applications", in *The solvent extraction of heptavalent technetium and rhenium by tributyl phosphate* (Oak Ridge National Laboratory, 1981).
- ⁶¹F. Kosinski and H. Bostian, "Lanthanum solvent extraction mechanisms using di-(2-ethylhexyl) phosphoric acid", *Journal of Inorganic and Nuclear Chemistry* **31**, 3623–3631 (1969).
- ⁶²A. Roca-Sabio, M. Mato-Iglesias, D. Esteban-Gómez, É. Tóth, A. d. Blas, C. Platas-Iglesias, and T. Rodríguez-Blas, "Macrocyclic receptor exhibiting unprecedented selectivity for light lanthanides", *Journal of the American Chemical Society* **131**, 3331–3341 (2009).
- ⁶³X. Sun, J. R. Bell, H. Luo, and S. Dai, "Extraction separation of rare-earth ions via competitive ligand complexations between aqueous and ionic-liquid phases", *Dalton Transactions* **40**, 8019 (2011).
- ⁶⁴E. Aluicio - Sarduy, N. A. Thiele, K. E. Martin, B. A. Vaughn, J. Devaraj, A. P. Olson, T. E. Barnhart, J. J. Wilson, E. Boros, and J. W. Engle, "Establishing radiolanthanum chemistry for targeted nuclear medicine applications", *Chemistry – A European Journal* **26**, 1238–1242 (2020).
- ⁶⁵A. A. Zamani, M. R. Yaftian, and N. Dallali, "Improved extraction-separation of lanthanum/ europium ions by bis(2-ethylhexyl)phosphoric acid using 12-crown-4 as an ion selective masking agent", *Iranian Journal of Chemistry and Chemical Engineering* **25**, 15–19 (2006).
- ⁶⁶HySS.
- ⁶⁷L. Alderighi, P. Gans, A. Ienco, D. Peters, A. Sabatini, and A. Vacca, "Hyperquad simulation and speciation (hyss): a utility program for the investigation of equilibria involving soluble and partially soluble species", *Coordination Chemistry Reviews* **184**, 311–318 (1999).
- ⁶⁸S. Aryal, *Ion exchange chromatography: principle, parts, steps, uses*, Sept. 2023.
- ⁶⁹S. Happel, "Vugm, part of the npl vcar conference", in *News radiopharmacy and other on-going r&d* (Triskem International).
- ⁷⁰Agilent, *An introduction to the fundamentals of inductively coupled plasma – mass spectrometry (icp-ms)*, Feb. 2024.
- ⁷¹J. Tom, *Uv-vis spectroscopy: principle, strengths and limitations and applications*, June 2021.
- ⁷²R. K. Biswas, M. A. Habib, and M. N. Islam, "Some physicochemical properties of (d2ehpa). 1. distribution, dimerization, and acid dissociation constants of d2ehpa in a kerosene/0.10 kmol m⁻³ (na⁺,h⁺)cl⁻ system and the extraction of mn(ii)", *Industrial & Engineering Chemistry Research* **39**, 155–160 (2000).
- ⁷³P.-C. Lee, C.-W. Li, J.-Y. Chen, Y.-S. Li, and S.-S. Chen, "Dissolution of d2ehpa in liquid–liquid extraction process: implication on metal removal and organic content of the treated water", *Water Research* **45**, 5953–5958 (2011).
- ⁷⁴A. Kumari, R. Panda, M. K. Jha, and D. D. Pathak, "Extraction of rare earth metals by organometallic complexation using pc88a", *Comptes Rendus Chimie* **21**, 1029–1034 (2018).
- ⁷⁵M. Gergoric, C. Ekberg, B.-M. Steenari, and T. Retegan, "Separation of heavy rare-earth elements from light rare-earth elements via solvent extraction from a neodymium magnet leachate and the effects of diluents", *Journal of Sustainable Metallurgy* **3**, 601–610 (2017).
- ⁷⁶D. Li, "Development course of separating rare earths with acid phosphorus extractants: a critical review", *Journal of Rare Earths* **37**, 468–486 (2019).
- ⁷⁷E. SMINČÁKOVÁ, L. KOMOROVÁ, and M. GÁLOVÁ, *Extraction of Rare Earth Metals by Bis(2-Ethylhexyl)phosphoric Acid* (1994).
- ⁷⁸M. T. Khaironie, M. Masturah, M. Y. Meor Sulaiman, and S. Nazaratul Ashifa, "Solvent extraction of light rare earth ions using d2ehpa from nitric acid and sulphuric acid solutions", *Advanced Materials Research* **970**, 209–213 (2014).
- ⁷⁹A. Rout and K. Binnemans, "Liquid–liquid extraction of europium(iii) and other trivalent rare-earth ions using a non-fluorinated functionalized ionic liquid", *Dalton Trans.* **43**, 1862–1872 (2014).
- ⁸⁰M. Bayyari, M. Nazal, and F. Khalili, "The effect of ionic strength on the extraction of thorium(iv) from perchlorate solution by didodecylphosphoric acid (hddpa)", *Arabian Journal of Chemistry* **3**, 115–119 (2010).

- ⁸¹J. Shibata and S. Nishimura, "Extraction of cu, ni and co with sodium salt of di-2-ethylhexylphosphoric acid", *Transactions of the Japan Institute of Metals* **23**, 614–619 (1982).
- ⁸²I. L. Dukov, A. F. Al-Nimri, and G. I. Kassabov, "Temperature effect on the solvent extraction of some lanthanides with thenoyltrifluoroacetone", *Monatshefte für Chemie / Chemical Monthly* **116**, 737–743 (1985).
- ⁸³A. Kandil, H. Aly, M. Raieh, and G. Choppin, "Temperature effects in synergistic solvent extraction", *Journal of Inorganic and Nuclear Chemistry* **37**, 229–232 (1975).
- ⁸⁴J. Wang, G. CHEN, S. Xu, Z. YIN, and Q. ZHANG, "Solvent extraction of rare earth ions from nitrate media with new extractant di-(2,3-dimethylbutyl)-phosphinic acid", *Journal of Rare Earths* **34**, 724–730 (2016).
- ⁸⁵J. Saien and S. Daliri, "Improving performance of liquid–liquid extraction with temperature for mass transfer resistance in both phases", *Journal of the Taiwan Institute of Chemical Engineers* **45**, 808–814 (2014).
- ⁸⁶N. Devi and B. Nayak, "Liquid-liquid extraction and separation of copper(II) and nickel(II) using LIX®984N", *Journal of the Southern African Institute of Mining and Metallurgy* **114**, 937–943 (2014).
- ⁸⁷S. M. Ibrahim, Y. Zhang, Y. Xue, S. Yang, F. Ma, Y. Gao, Y. Zhou, and G. Tian, "Selective extraction of light lanthanides(iii) by n,n-di(2-ethylhexyl)-diglycolamic acid: a comparative study with n,n-dimethyl-diglycolamic acid as a chelator in aqueous solutions", *ACS Omega* **4**, 20797–20806 (2019).
- ⁸⁸J. M. Arnold and E. O. Otu, "Effect of temperature on the synergistic extraction of some lanthanides by 2ethylhexyl phenylphosphonic acid and micelles of dinonyl naphthalene sulfonic acid", *Solvent Extraction and Ion Exchange* **22**, 415–428 (2004).
- ⁸⁹M. R. Yaftian and M. Vahedpour, "Influence of the temperature on the solvent extraction of some lanthanide picrates by a phosphorylated calix[4]arene", *Phosphorus Sulfur and Silicon and The Related Elements - PHOSPHOR SULFUR SILICON* **174**, 93–100 (2001).
- ⁹⁰I. L. Dukov, "Temperature effect on the synergistic solvent extraction of some lanthanides with mixtures of 1-phenyl-3-methyl-4-benzoyl-pyrazol-5-one and aliquat 336", *Hydrometallurgy* **44**, 21–27 (1997).
- ⁹¹Y. Jin, Y. Ma, Y. Weng, X. Jia, and J. Li, "Solvent extraction of fe³⁺ from the hydrochloric acid route phosphoric acid by d2ehpa in kerosene", *Journal of Industrial and Engineering Chemistry* **20**, 3446–3452 (2014).
- ⁹²E. Borai, A. Shahr EIDin, E. El Afifi, R. Aglan, and M. Abo-Aly, "Subsequent separation and selective extraction of thorium (iv), iron (iii), zirconium (iv) and cerium (iii) from aqueous sulphate medium. e.h. borai, a.m. shahr el-din, e.m. el afifi, r.f. aglan and m.m. abo-aly, south african journal of chemistry 69, pp. 148-156 (2016). (doi: <http://dx.doi.org/10.17159/0379-4350/2016/v69a18>)", *South African journal of chemistry. Suid-Afrikaanse tydskrif vir chemie* **69**, 148–156 (2016).
- ⁹³A. Jezuita, P. Wiczorkiewicz, H. Szatyłowicz, and T. Krygowski, "Solvent effect on the stability and reverse substituent effect in nitropurine tautomers", *Symmetry* **13**, 1223 (2021).
- ⁹⁴Y. El-Nadi, "Effect of diluents on the extraction of praseodymium and samarium by cyanex 923 from acidic nitrate medium", *Journal of Rare Earths* **28**, 215–220 (2010).
- ⁹⁵A. I. Vogel, B. S. Furniss, A. J. Hannaford, G. P. W. Smith, and A. R. Tatchell, *Vogel's textbook of practical organic chemistry. 5th ed*, 5th ed. (Longman, 1989).
- ⁹⁶S. Budiman, A. Hardian, L. Virdasari, N. Nurdeni, H. Herman, A. Mutalib, A. Anggraeni, and H. H. Bahti, "Separation of gadolinium(iii) from terbium(iii) by the liquid-liquid extraction method with dibutyl-dithiophosphate as the extractant", *Journal of Tropical Pharmacy and Chemistry* **6**, 10.25026/jtpc.v6i1.430 (2022).
- ⁹⁷S. Radhika, V. Nagaraju, B. Nagaphani Kumar, M. L. Kantam, and B. R. Reddy, "Solvent extraction and separation of rare-earths from phosphoric acid solutions with tops 99", *Journal of Rare Earths* **30**, 1270–1275 (2012).

- ⁹⁸L. Koekemoer, M. Badenhorst, and R. Everson, "Determination of viscosity and density of di-(2-ethylhexyl) phosphoric acid + aliphatic kerosene", *Journal of Chemical and Engineering Data - J CHEM ENG DATA* **50**, 10.1021/je0496645 (2005).
- ⁹⁹O. Cheremisina, V. Sergeev, A. Fedorov, and D. Alferova, "Concentration and separation of heavy rare-earth metals at stripping stage", *Metals* **9**, 10.3390/met9121317 (2019).
- ¹⁰⁰K. Mohamed Takip, M. Markom, and M. Y. Meor Sulaiman, "Solvent extraction of light rare earths from acidic medium by di-(2-ethylhexyl) phosphoric acid in kerosene", *Jurnal Kejuruteraan* **27**, 57–62 (2015).
- ¹⁰¹W. Zhang and R. Honaker, "Process development for the recovery of rare earth elements and critical metals from an acid mine leachate", *Minerals Engineering* **153**, 10.1016/j.mineng.2020.106382 (2020).
- ¹⁰²K. N. Han, "Characteristics of precipitation of rare earth elements with various precipitants", *Minerals* **10**, 10.3390/min10020178 (2020).
- ¹⁰³P. A. Lessing and A. W. Erickson, "Synthesis and characterization of gadolinium phosphate neutron absorber", *Journal of the European Ceramic Society* **23**, 3049–3057 (2003).
- ¹⁰⁴C. J. B. Edward W. Wilde and M. B. Goli, "Method for removing gadolinium from used heavy water reactor moderator", *Nuclear Technology* **144**, 141–143 (2003).



Results

Table A.1: Extraction efficiencies [%] of Tb and Gd for various extractants at pH = 1.3. The extractions were carried out with 15 mM Gd and 0.15 mM Tb in HNO₃ as the aqueous phase, PE 100-140 as the organic phase and 10 min vortexing time. The concentrations of the extractants are 0.1 M DEHPA, 0.5 M PC-88A and 0.1 M DDPA with 2 % v/v TBP. The error represents one standard deviation of the mean.

Extractant	EE Tb [%]	EE Gd [%]
DEHPA	98.3 ± 0.5	85.7 ± 5.5
PC-88A	98.6 ± 0.2	96.7 ± 3.0
DDPA + TBP	73.6 ± 2.5	47.8 ± 1.5

Table A.2: Extraction efficiency [%] of Tb for DEHPA and PC-88A at pH = 1.3 versus extractant concentration. All extractions were carried out with 15 mM Gd and 0.15 mM Tb in HNO₃ as the aqueous phase, PE 100-140 as the organic phase and 10 min vortexing time. The error represents one standard deviation of the mean.

Extractant	0.05 M	0.1 M	0.5 M
DEHPA	52.8 ± 0.1	98.3 ± 0.5	96.8 ± 1.8
PC-88A	53.4 ± 0.4	84.6 ± 0.3	98.6 ± 0.2

Table A.3: Extraction efficiencies [%] of Tb and Gd for 0.1 M DEHPA and 0.5 M PC-88A versus pH. All extractions were carried out with 15 mM Gd and 0.15 mM Tb in HNO₃ as the aqueous phase, PE 100-140 as the organic phase and 10 min vortexing time. The error represents one standard deviation of the mean.

pH	DEHPA		PC-88A	
	EE Tb [%]	EE Gd [%]	EE Tb [%]	EE Gd [%]
1.0	92.2 ± 2.4	71.1 ± 3.2	90.0 ± 1.1	70.8 ± 2.8
1.2	97.6 ± 0.2	87.6 ± 1.4	97.3 ± 0.1	95.8 ± 2.5
1.3	98.3 ± 0.5	85.7 ± 5.5	98.6 ± 0.2	96.7 ± 3.0

Table A.4: Extraction efficiencies [%] of Tb and Gd using 0.1 M DEHPA at various pH values. The extractions were carried out with 15 mM Gd and 0.15 mM Tb in HNO₃ as the aqueous phase, PE 100-140 as the organic phase and 10 min vortexing time. The error represents one standard deviation of the mean.

pH	0.1	1.0	1.2	1.3	1.5 / 1.6	2.0 / 2.2	2.5 / 3.0	5.0
EE Tb [%]	13.9 ± 0.1	92.2 ± 1.1	97.6 ± 1.3	98.3 ± 0.5	97.2 ± 0.7	95.2 ± 0.3	95.7 ± 0.3	96.5 ± 2.0
EE Gd [%]	7.7 ± 3.4	71.1 ± 3.2	87.6 ± 1.4	85.7 ± 5.5	87.3 ± 5.0	91.7 ± 1.5	94.9 ± 2.0	95.4 ± 2.2

Table A.5: Extraction efficiencies [%] of Tb and Gd using 0.1 M DEHPA and aqueous phase at pH = 1.3. The extractions were carried out with 15 mM Gd and 0.15 mM Tb in HNO₃, PE 100-140 as the organic phase and various vortexing times. The error represents one standard deviation of the mean.

Vortexing time	30 seconds	1 min	3 min	5 min	10 min
EE Tb [%]	95.5 ± 1.5	95.9 ± 1.6	96.8 ± 0.3	97.42 ± 0.04	98.3 ± 0.5
EE Gd [%]	89.8 ± 1.4	90.4 ± 0.6	-	-	85.7 ± 5.5

Table A.6: Extraction efficiency [%] of Tb using 0.1 M DEHPA in chloroform or PE 100-140 with aqueous phase HNO₃ at pH = 1.3. The extractions were carried out with 15 mM Gd and 0.15 mM Tb and 10 minutes vortexing time. The error represents one standard deviation of the mean.

Organic phase	EE Tb [%]
PE 100-140	98.3 ± 0.5
Chloroform	64.6 ± 0.4

Table A.7: Extraction efficiency [%] of Tb and Gd using 0.1 M DEHPA in PE 100-140 with aqueous phase HNO₃ or HCl at pH = 1.3. The extractions were carried out with 15 mM Gd and 0.15 mM Tb and 10 minutes vortexing time. The error represents one standard deviation of the mean.

Aqueous phase	EE Tb [%]	EE Gd [%]
HNO ₃	98.3 ± 0.5	85.7 ± 5.5
HCl	88.6 ± 3.2	85.5 ± 2.1

Table A.8: The result of a speciation simulation in CHEAQS. The used parameters are: [Tb³⁺] = 0.15 mM, [Gd³⁺] = 15 mM, [H⁺] = 0.05 M, [NO₃⁻] = 68.8 mM, 18.8 mM and 68.8 mM, [Cl⁻] = 28.1 mM, 78.1 mM and 28.1 mM, [Na⁺] = 0 M, 0 M and 0.5 M and the values given are relative to the initial concentration Gd/Tb added to the solution.

Species	HNO ₃	HCl	HNO ₃ + NaOH
Free Tb ³⁺	89.73 %	95.97 %	92.26 %
TbNO ₃ ²⁺	10.25 %	3.93 %	7.72 %
TbCl ²⁺	0.02 %	0.09 %	0.02 %
Free Gd ³⁺	94.20 %	97.73 %	95.68 %
GdNO ₃ ²⁺	5.77 %	2.14 %	4.30 %
GdCl ²⁺	0.03 %	0.11 %	0.02 %

Table A.9: Extraction efficiencies [%] of Tb and Gd. The extractions were carried out with 150 mM Gd and 0.15 mM Tb in HNO₃ as the aqueous phase at pH = 1.3. Various concentrations of DEHPA in PE 100-140 were used as the organic phase and the vials were vortexed for 10 minutes. The error represents one standard deviation of the mean.

DEHPA concentration [mol/L]	0.05	0.2	0.5	1.0
EE Tb [%]	53.1 ± 0.4	66.0 ± 0.6	85.7 ± 1.2	93.4 ± 0.5
EE Gd [%]	28.9 ± 7.1	34.1 ± 3.2	63.3 ± 1.2	77.1 ± 5.8

Table A.10: BEE [%] of Tb with various concentrations HNO₃ and HCl as the back-extracting agent. The error represents one standard deviation of the mean.

Concentration BE agent [mol/L]	1	1.5	2	3	4	5
HNO ₃	79.2 ± 3.6	95.2 ± 0.1	98.2 ± 0.1	99.39 ± 0.04	99.5 ± 0.2	99.77 ± 0.01
HCl	81.5 ± 1.4	-	98.2 ± 0.2	-	-	-

Table A.11: The results of extractions using 0.005 M MACROPA and 0.001 M DEHPA and back-extraction with 2 M HNO₃ for 100x diluted Tb/Gd aqueous solution at pH 2 and pH 3.5, a vortexing time of 10 min and PE 100-140 as the organic phase. The error represents one standard deviation of the mean.

pH	EE Tb [%]	EE Gd [%]
2.0	90.1 ± 1.7	61.9 ± 1.5
3.5	95.0 ± 0.2	53.1 ± 3.0

Table A.12: The results of extractions using MACROPA and 0.001 M DEHPA and back-extraction with 2 M HNO₃ for 100x diluted Tb/Gd aqueous solution at pH 3.5, a vortexing time of 10 min and PE 100-140 as the organic phase versus various concentrations of MACROPA. The error represents one standard deviation of the mean.

MACROPA concentration [mol/L]	EE Tb [%]	EE Gd [%]
0.001	96.3 ± 1.8	75.8 ± 1.7
0.005	95.0 ± 0.2	53.1 ± 3.0
0.01	93.4 ± 2.7	58.9 ± 2.3

Table A.13: The results of repeating the MACROPA/DEHPA extraction system: 0.005 M MACROPA and 0.001 M DEHPA, back-extraction with 2 M HNO₃ for 100x diluted Tb/Gd aqueous solution at pH 3.5 as a starting solution, a vortexing time of 10 min and PE 100-140 as the organic phase. Values given are total EEs after each step.

Extraction #	0	1	2	3
EE Tb [%]	100	56.0	34.8	19.8
EE Gd [%]	100	21.2	7.3	2.6

Table A.14: The results of repeating the MACROPA/DEHPA extraction system: 0.005 M MACROPA and 0.001 M DEHPA, back-extraction with 2 M HNO₃ for 100x diluted Tb/Gd aqueous solution at pH 3.5 as a starting solution, a vortexing time of 10 min and PE 100-140 as the organic phase. Values shown are EEs for each extraction.

Extraction #	1	2	3
EE Tb [%]	56.0	62.2	56.8
EE Gd [%]	21.2	34.3	36.3

B

Data Analysis

B.1. ICP-MS Data Analysis

The ICP-MS returns measured concentrations of its samples in μg . It does this by calibration of samples with known concentrations. Usually several of these reference samples are measured to create a calibration plot of counts vs known concentration for each element. The calibration plots of Tb and Gd are shown in Figure B.1. The calibrations at lower concentrations (0 - 5 ppb) are not very good. As this is our range of measurement for Tb we use radioactive Tb and gamma counting for Tb EE measurements. The calibrations for Gd in the range we are interested in (300 - 500 ppb) are good, the relative error is not more than a percent.

To calculate the EEs, the concentrations of the samples before and after the extraction were corrected for dilution and used as input in Equation 2.2 replacing the activity.

B.2. Wallac Data Analysis

The Wallac gamma counter returns the number of counts of a measurement over a certain time period. These counts are corrected for decay and the weight of the vials using the measured average density of the respective phase. The EEs are then calculated using Equation 2.3. This equation is used instead of Equation 2.2 because measurement results on the Wallac are influenced by the sample volume. As the measured organic and aqueous phases have equal volume this is not a problem, but if the total activity (which has higher volume) were to be measured this would influence the results. All calculations of the EEs were done with Python.

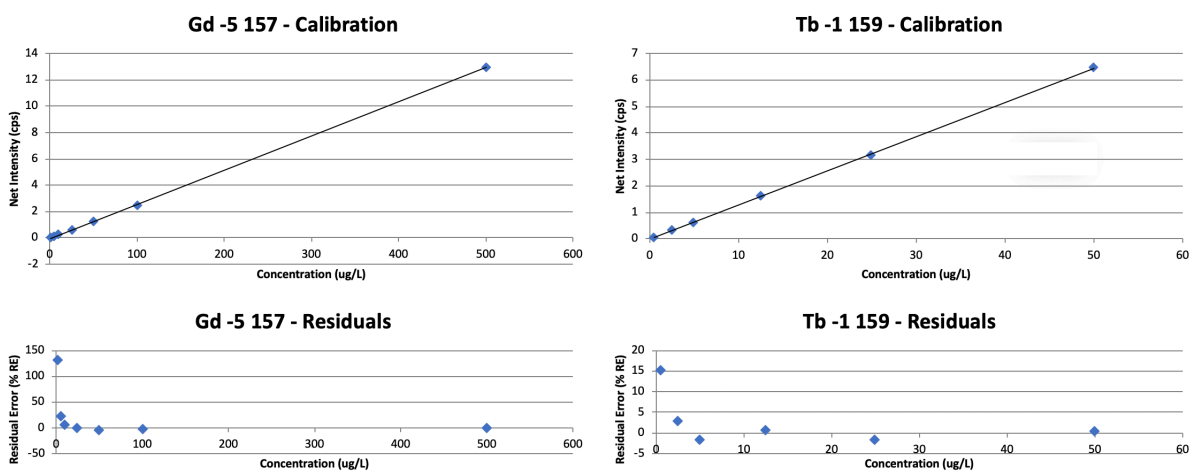


Figure B.1: The ICP-MS calibration and residual error plots. The calibration at higher ppb is better for both Tb and Gd.